N76-10196

NASA TECHNICAL
MEMORANDUM

NASA TM X-62,444

NASA TM X-62,444

SHADOWGRAPHS OF AIR FLOW OVER PROSPECTIVE SPACE SHUTTLE CONFIGURATIONS AT MACH NUMBERS FROM 0.8 TO 1.4

Jules B. Dods, Jr., Richard D. Hanly and James H. Efting

Ames Research Center
Moffett Field, Ca. 94035

May 1975

DMS-DR-2255
(TM X-62, 444)

The attached document presents results of wind tunnel investigations conducted by NASA/ARC and placed in the Space Shuttle data system. Additional copies may be obtained from Chrysler Data Management Services by referring to the DMS-DR designation.

Distributed under NASA Contract Number NAS9-13247

by

Data Management Services
Chrysler Corporation Space Division

for

Engineering Analysis Division

Johnson Space Center
National Aeronautics and Space Administration
Houston, Texas

FACILITY COORDINATOR:

S. L. Treon
Mail Stop 227-5
Ames Research Center
Moffett Field, California 94035

Phone: 415-965-5852

PROJECT ENGINEERS:

Jules B. Dods, Jr.,
Richard D. Hanly, and
James H. Efting
Mail Stop 227-9
Ames Research Center
Moffett Field, California 94035

Phone: 415-965-6215

DATA MANAGEMENT SERVICES:

Prepared by: Liaison--T. L. Mulkey
Operations--Maurice Moser, Jr.

Reviewed by: G. G. McDonald, J. L. Glynn

Approved: N. D. Kemp, Manager
Data Management Services

Concurrence: J. G. Swider, Manager
Flight Technology Branch

Chrysler Corporation Space Division assumes responsibility only for printing and distributing this document.

SHADOWGRAPHS OF AIR FLOW OVER PROSPECTIVE SPACE SHUTTLE CONFIGURATIONS AT MACH NUMBERS FROM 0.8 TO 1.4

By Jules B. Dods, Jr., Richard D. Hanly and James H. Efting

Ames Research Center

SUMMARY

Shadowgraphs of five Space Shuttle Launch configurations are presented. The model was a 4 percent-scale Space Shuttle Vehicle, tested in the 11- by 11-foot Transonic Wind Tunnel at Ames Research Center. The Mach number was varied from 0.8 to 1.4 with three angles of sideslip (0°, 5° and -5°) that were used in conjunction with three angles of attack (4°, -4°, and 0°). The model configurations included both series-burn and parallel-burn configurations, two canopy configurations, two positions of the Orbiter nose relative to the HO tank nose, and two HO tank nose-cones angles (15° and 20°). The data consist entirely of shadowgraph photographs.

INTRODUCTION

Preliminary data results have been presented for the investigation of the aerodynamic performance of a 4 percent-scale model of the MSC Space Shuttle vehicle in references 1 and 2. In addition to the fluctuating pressure data of those reports, shadowgraphs were also taken during the course of the tests. The purpose of these photographs was to identify and locate zones of significant turbulence in order that unsteady pressure instrumentation could be best located to measure maximum values. Although additional tests will be needed when a final Space Shuttle configuration is selected, early tests of candidate configurations are also useful to gain insight on the complexities of the flow and to acquire preliminary estimates of the fluctuating pressures. The present report should be considered as a supplement to reference 2 in order to complete the documentation of those tests, and as such the discussion of results presented herein will be very brief.

NOTATION

HO	hydrogen-oxygen tank
SRM	solid rocket motors
TWT	transonic wind tunnel
M_∞	free stream Mach number
q_∞	free stream dynamic pressure
α	angle of attack, deg.
β	angle of sideslip, deg.

CONFIGURATION DESCRIPTION

Of the seven Space Shuttle configurations reported in reference 2, only five of them were tested in the Mach number range of the 11- by 11-ft TWT. The other two configurations (no's 6 and 7) were tested only in the 9- by 7-foot SWT to determine the effect of highly underexpanded rocket exhaust plumes and Orbiter engines using solid-body plumes for simulation at free-stream Mach numbers of 1.6 and 2.2. Configuration 5 showing typical dimensional information is shown in figure 1. A detailed description of the configurations tested is shown in figure 2. Installation photographs of each configuration are presented in reference 2 along with a more detailed description of the various configurations.

RESULTS AND DISCUSSION

The data presented herein consist of shadowgraph air-flow studies of five configurations of a 4 percent-scale model of the Space Shuttle Vehicle. In general, the data are presented for each configuration at free-stream Mach numbers from 0.80 to 1.40 at angles of sideslip of 0° and 5° in combination with angles of attack of -4°, 0°, and 4°. An exception to this is for configuration 5 wherein the results are for angles of attack and sideslip of (0°, 0°), (8°, -5), or (4°, -5°) respectively.

The shadowgraphs are presented in figures 3 through 6 for configuration 1, in figures 7 through 11 for configuration 2, and in figures 12 through 17 for configuration 3. The effect of changing the canopy can be seen by comparing the photographs of configuration 3 with those of configuration 4 in figures 18 through 22. The remainder of the data are for the parallel-burn configuration (no. 5) in figures 23 through 25. Although some shadowgraphs are listed for the same testing conditions, they are not duplicates since the model was raised or lowered in the tunnel to present a different field of view.

For convenience, a detailed listing of the figures is given in Table I.

CONCLUDING REMARKS

Data in the form of shadowgraph photographs are presented to aid in the identification and location of regions of significant turbulence. The data are considered to be supplemental to fluctuating pressure data previously reported for this test and are presented primarily to complete the documentation of that work.

Ames Research Center
National Aeronautics and Space Administration
Moffett Field, California 94035

May 2, 1975

REFERENCES

1. Dods, Jules B. Jr.; Hanly, Richard D.: In-Flight Aeroacoustic Environments on Prospective Space Shuttle Vehicles. NASA Space Shuttle Technology Conference. NASA TMX 2570, pp. 71-96, July 1972.

2. Dods, Jules B. Jr.; Hanly, Richard D.; Efting, James H.: Overall Fluctuating Pressure Levels on Prospective Space Shuttle Configurations at Mach Numbers from 0.8 to 2.2. NASA TM X-62,280, April 1973.

TABLE 1. - LIST OF FIGURES

TABLE 1. - LIST OF FIGURES - Continued.

TABLE 1. - LIST OF FIGURES - Continued.

TABLE 1. - LIST OF FIGURES - Concluded.

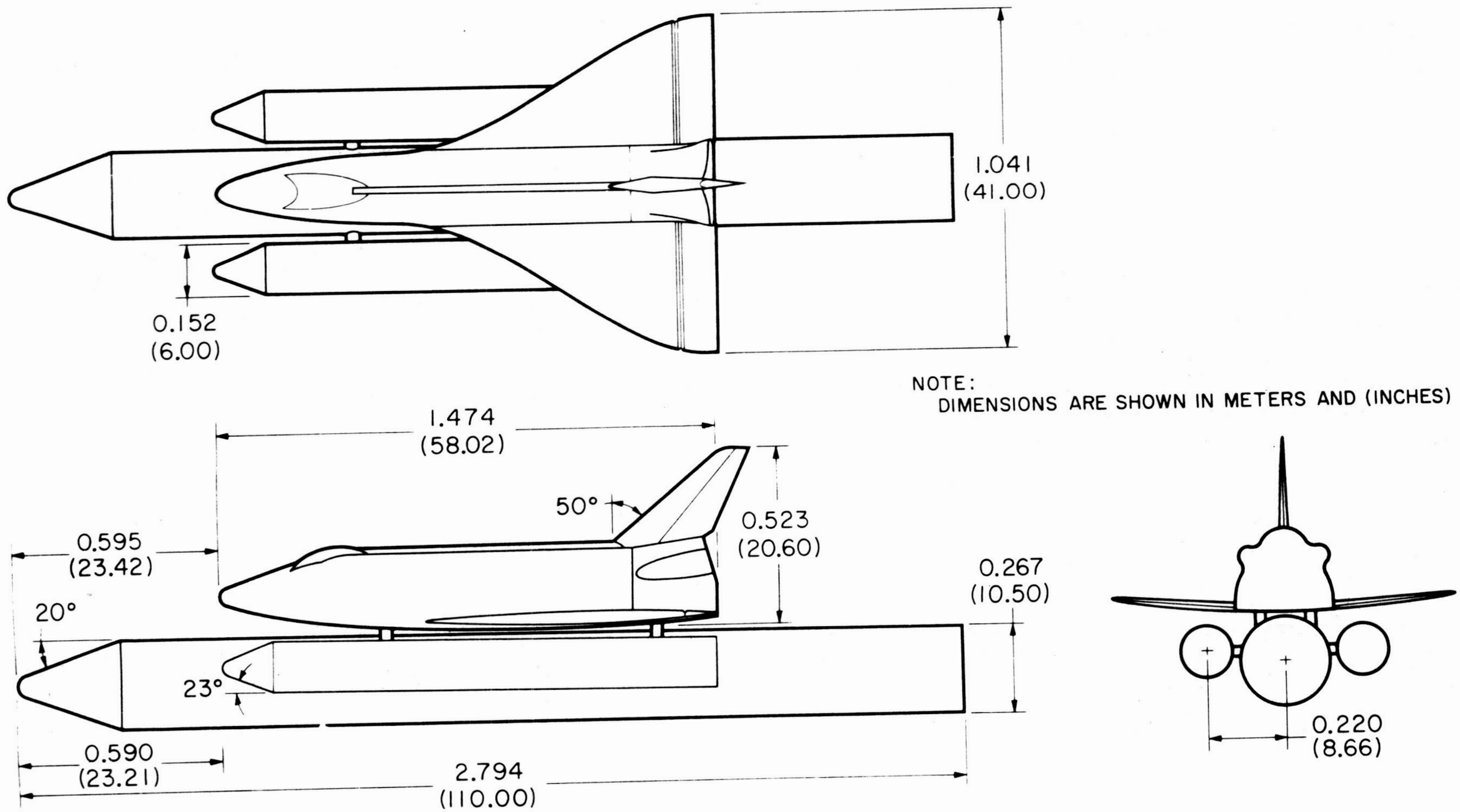

Figure 1. PARALLEL-BURN CONFIGURATION WITH MODIFIED CANOPY.

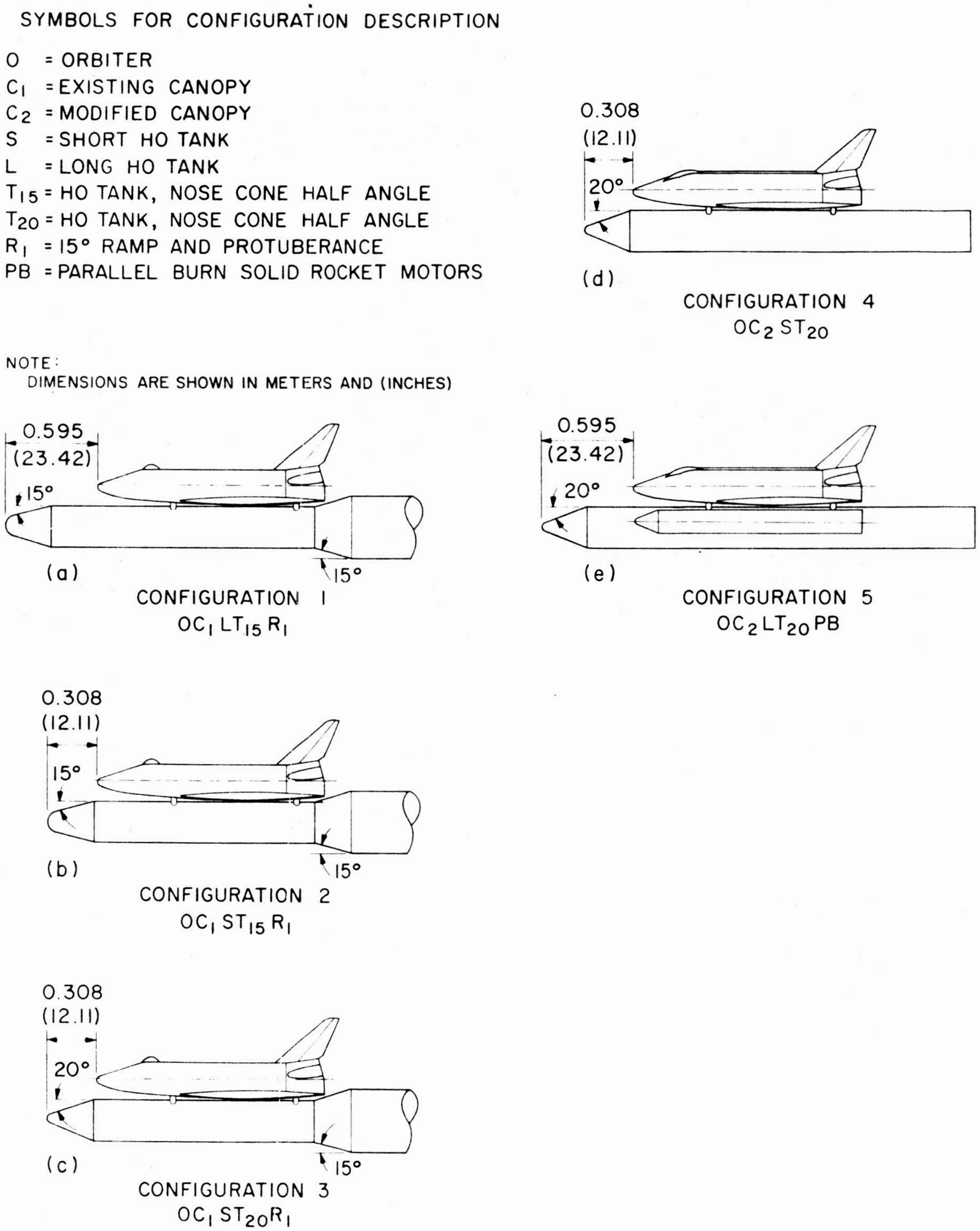

Figure 2.- Configurations tested.

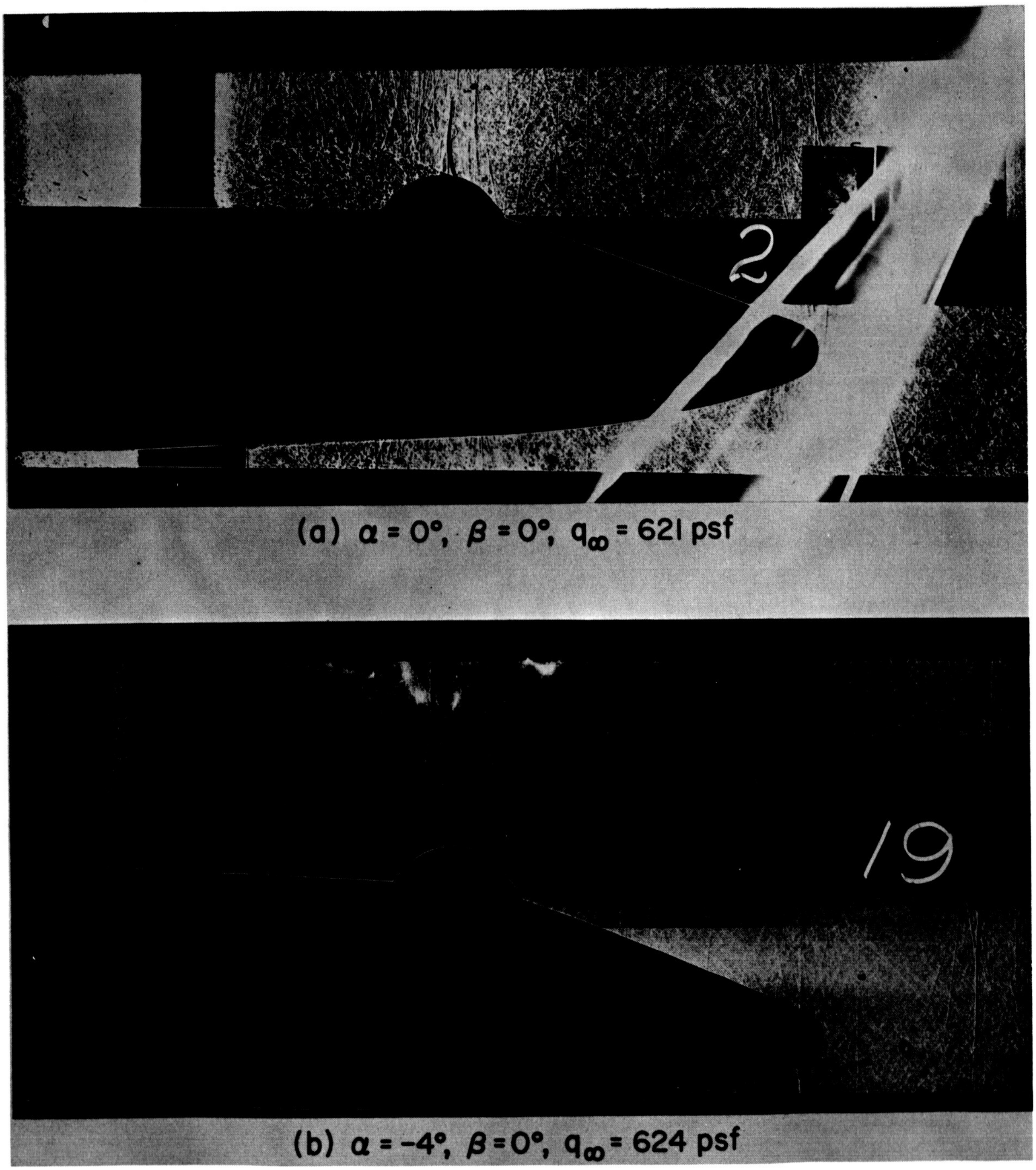

(a) $\alpha = 0°$, $\beta = 0°$, $q_\infty = 621$ psf

(b) $\alpha = -4°$, $\beta = 0°$, $q_\infty = 624$ psf

Figure 3. - Shadowgraphs of series-burn configuration 1 at $M_\infty = 0.80$.

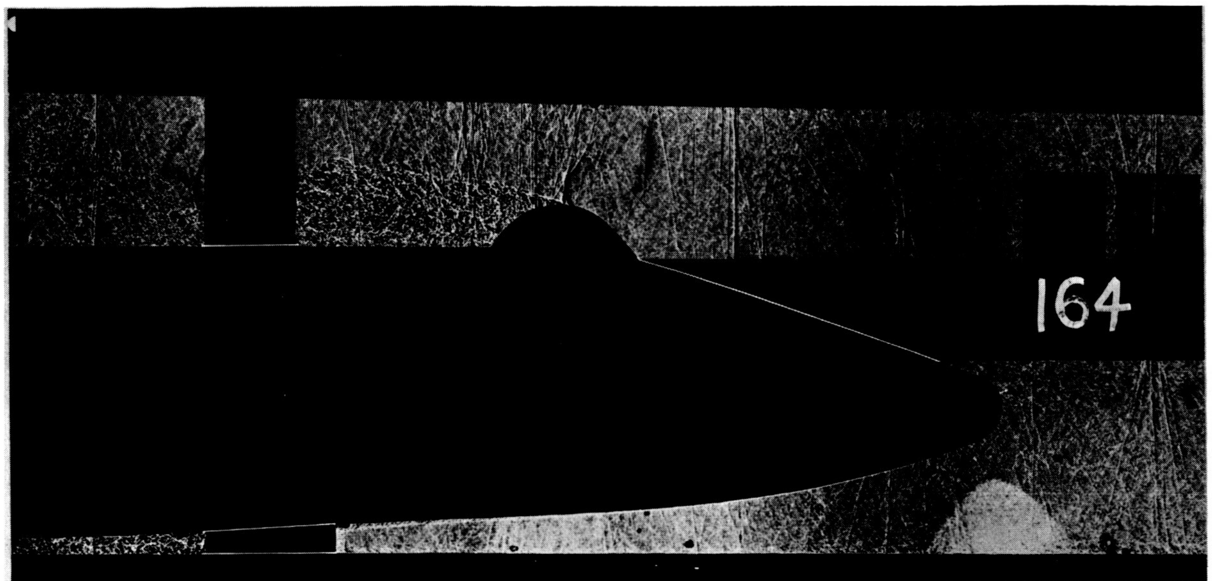

(c) $\alpha = 0°$, $\beta = 0°$, $q_\infty = 622$ psf

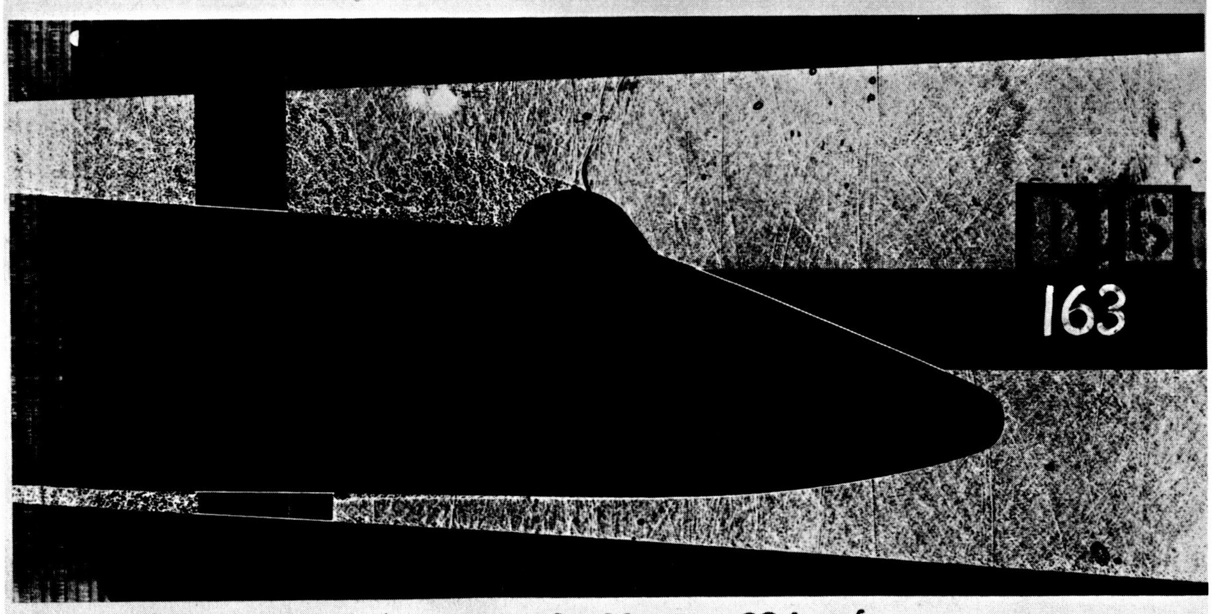

(d) $\alpha = -4°$, $\beta = 0°$, $q_\infty = 624$ psf

Figure 3. - Continued.

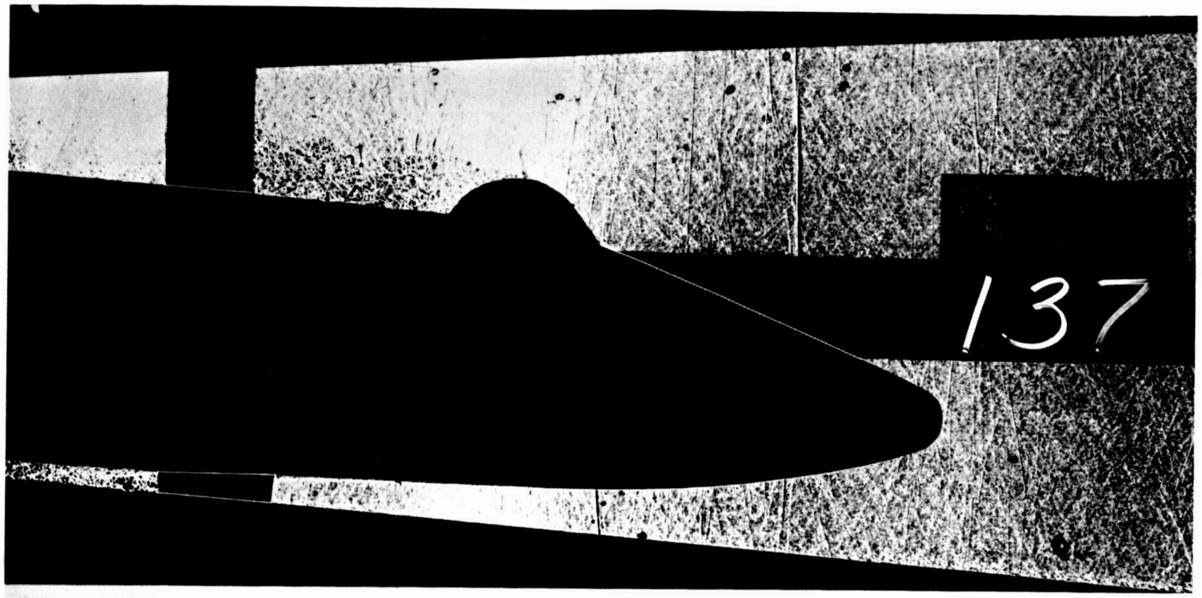

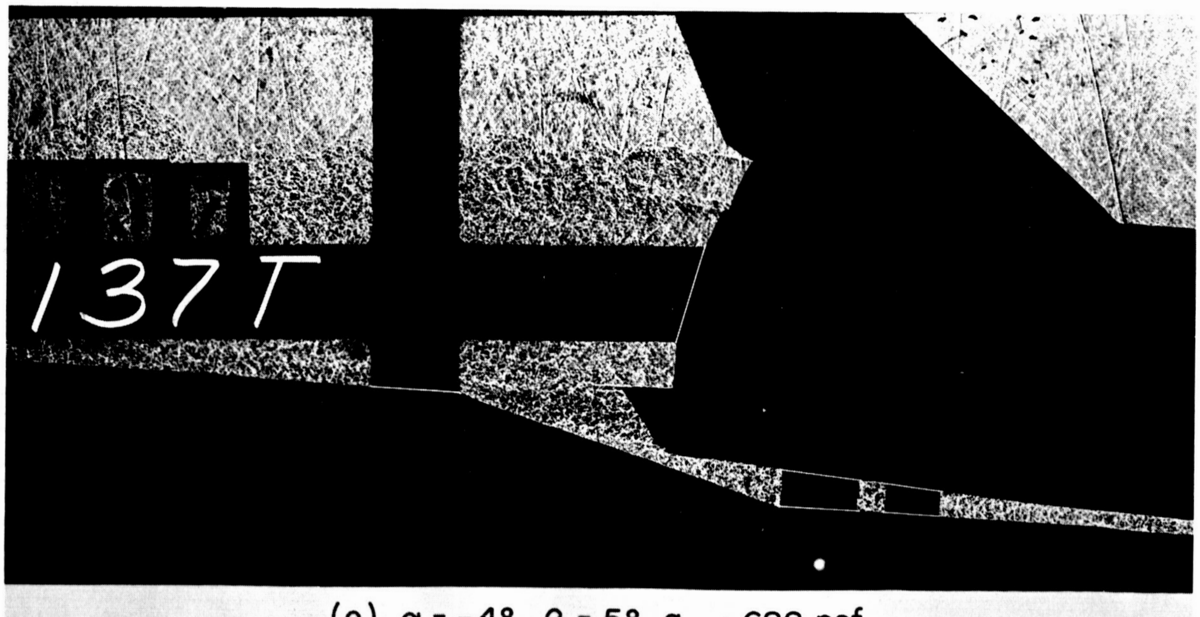

(e) $\alpha = -4°$, $\beta = 5°$, $q_\infty = 622$ psf

Figure 3. - Continued.

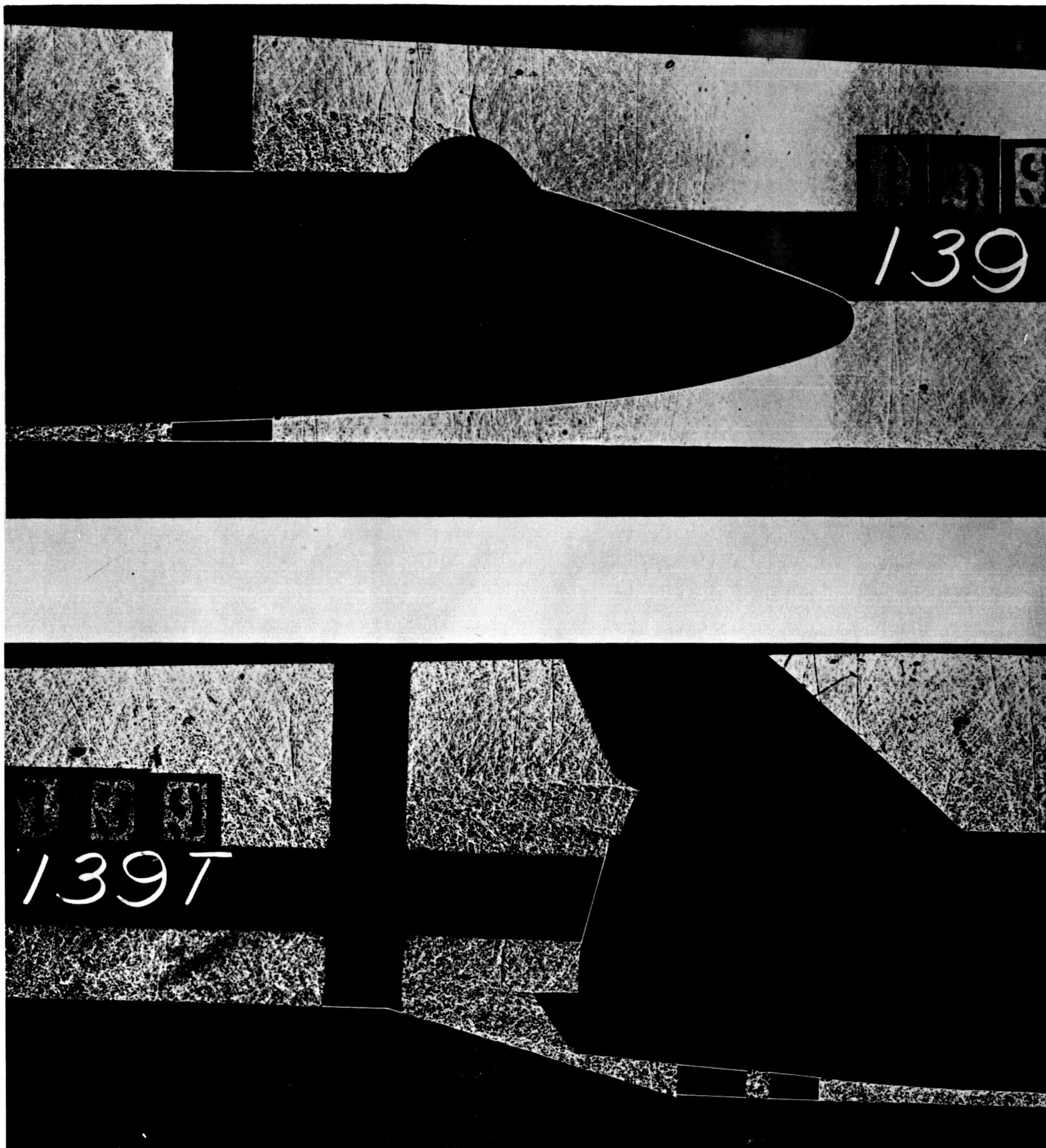

(f) $\alpha = 0°$, $\beta = 5°$, $q_\infty = 625$ psf

Figure 3. - Continued.

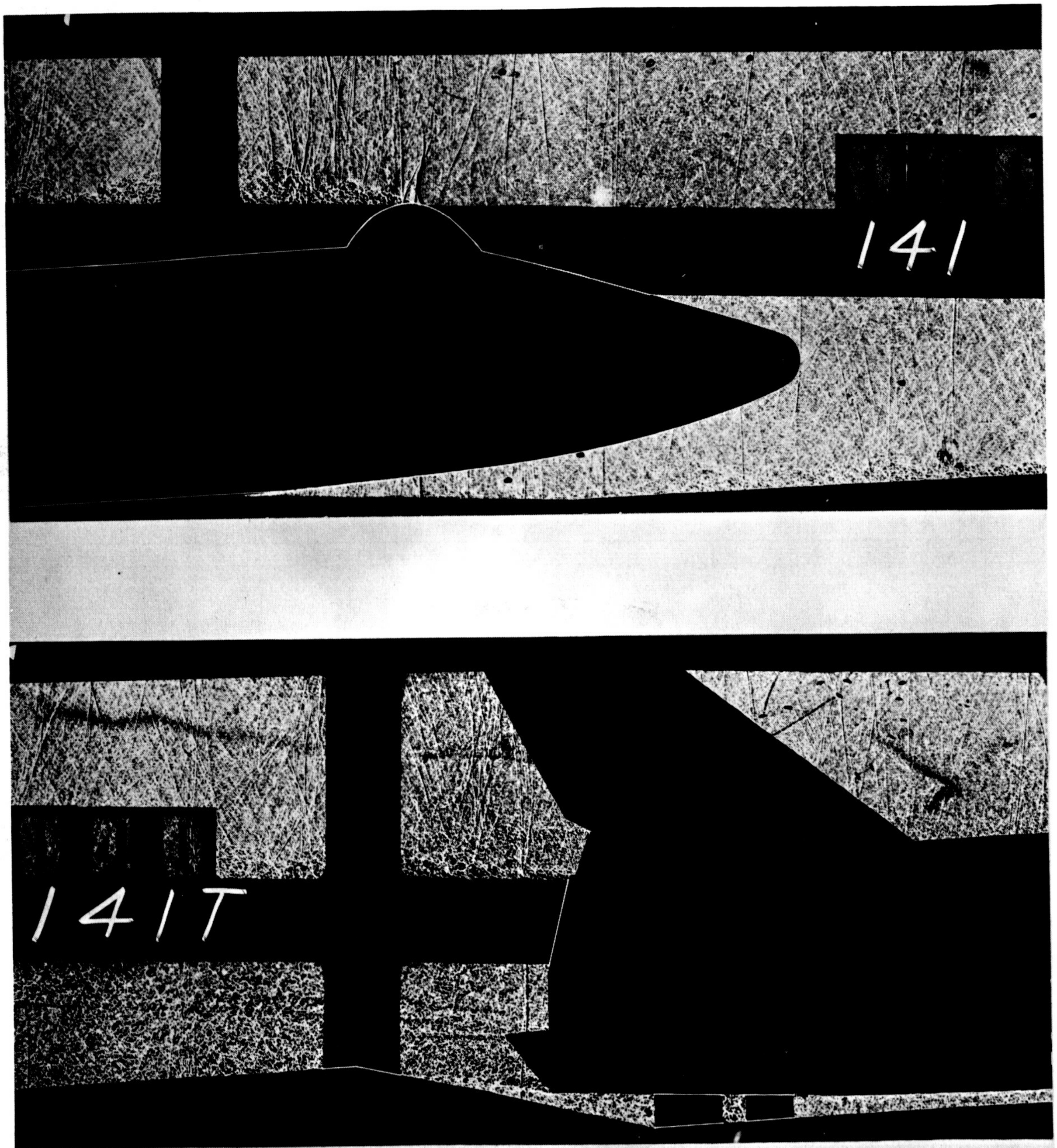

(g) $\alpha = 4°$, $\beta = 5°$, $q_{\infty} = 623$ psf

Figure 3. - Continued.

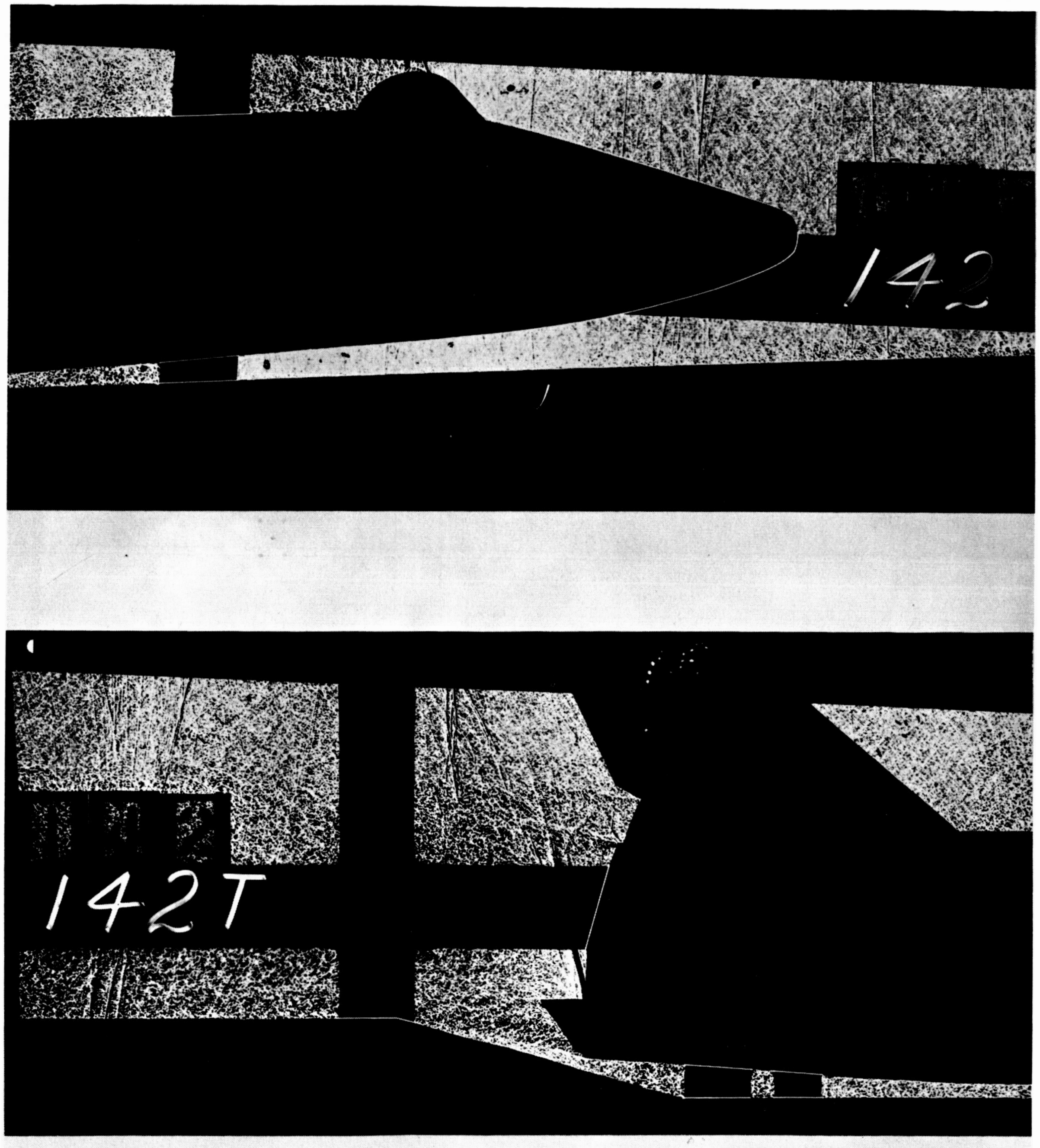

(h) α = 4°, β = 5°, q_{∞} = 623 psf

Figure 3. - Concluded.

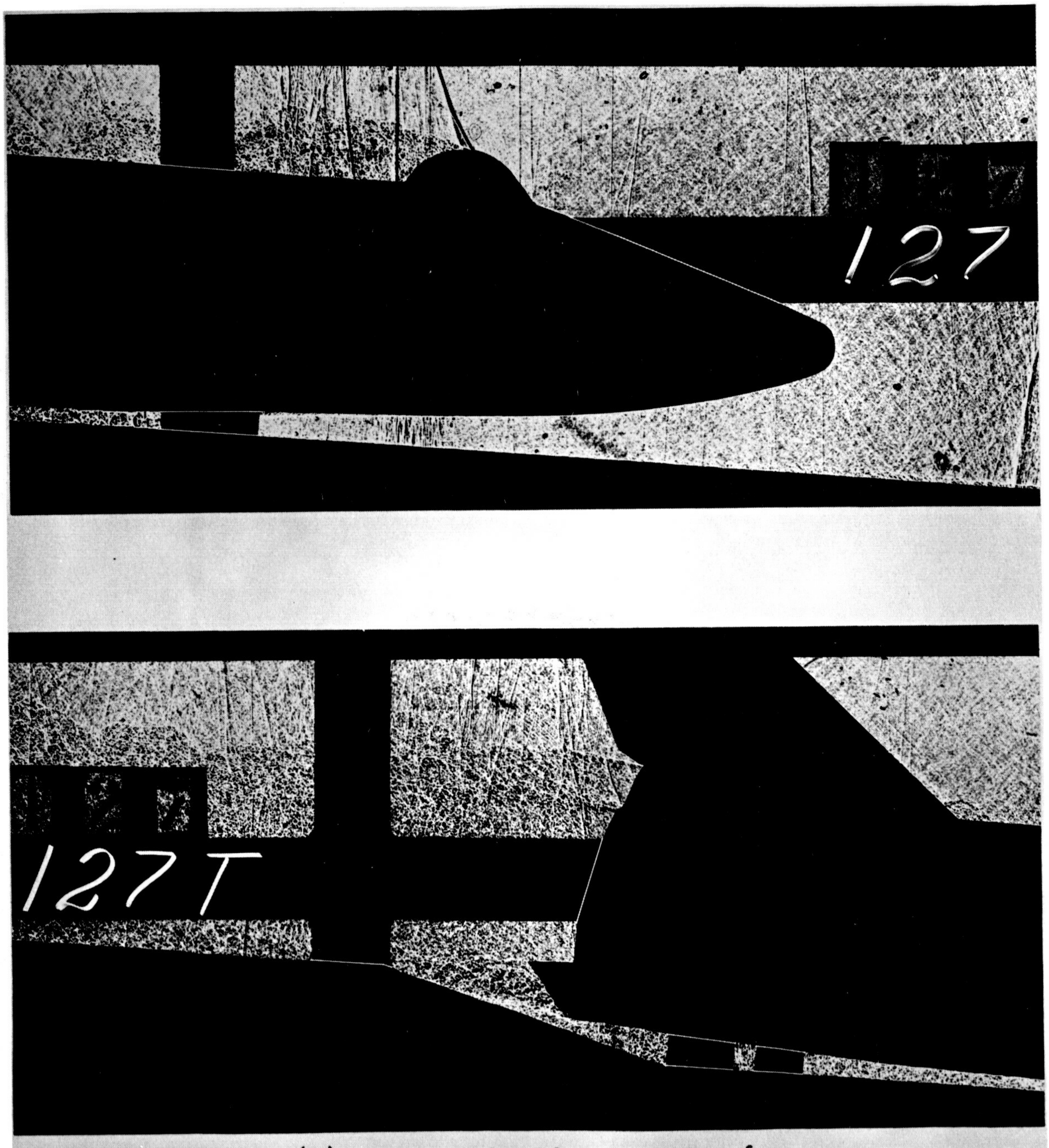

(a) $\alpha = -4°$, $\beta = 5°$, $q_\infty = 713$ psf

Figure 4. - Shadowgraphs of series-burn configuration 1 at $M_\infty = 0.90$.

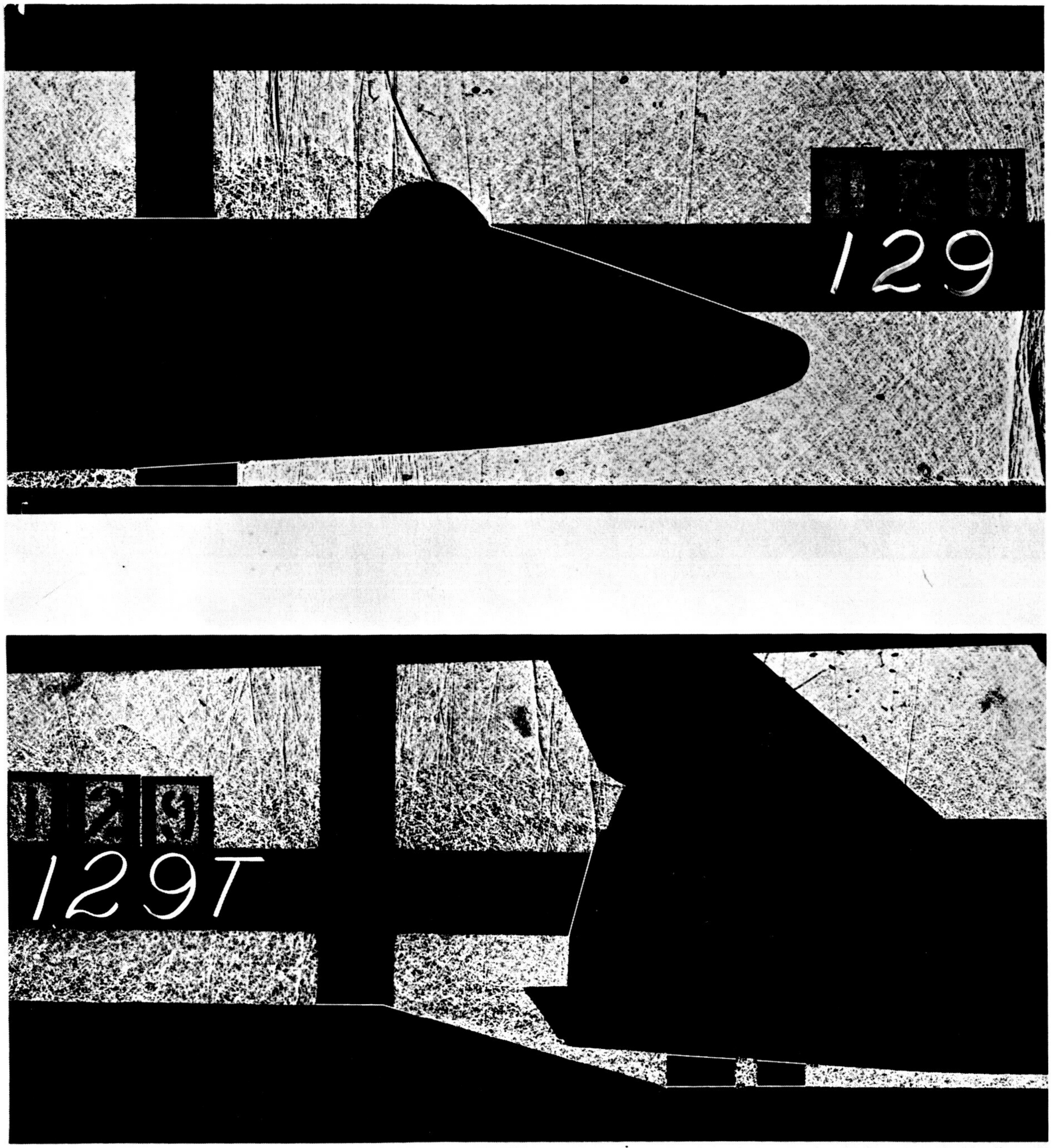

(b) $\alpha = 0°$, $\beta = 5°$, $q_{\infty} = 711$ psf

Figure 4. - Continued.

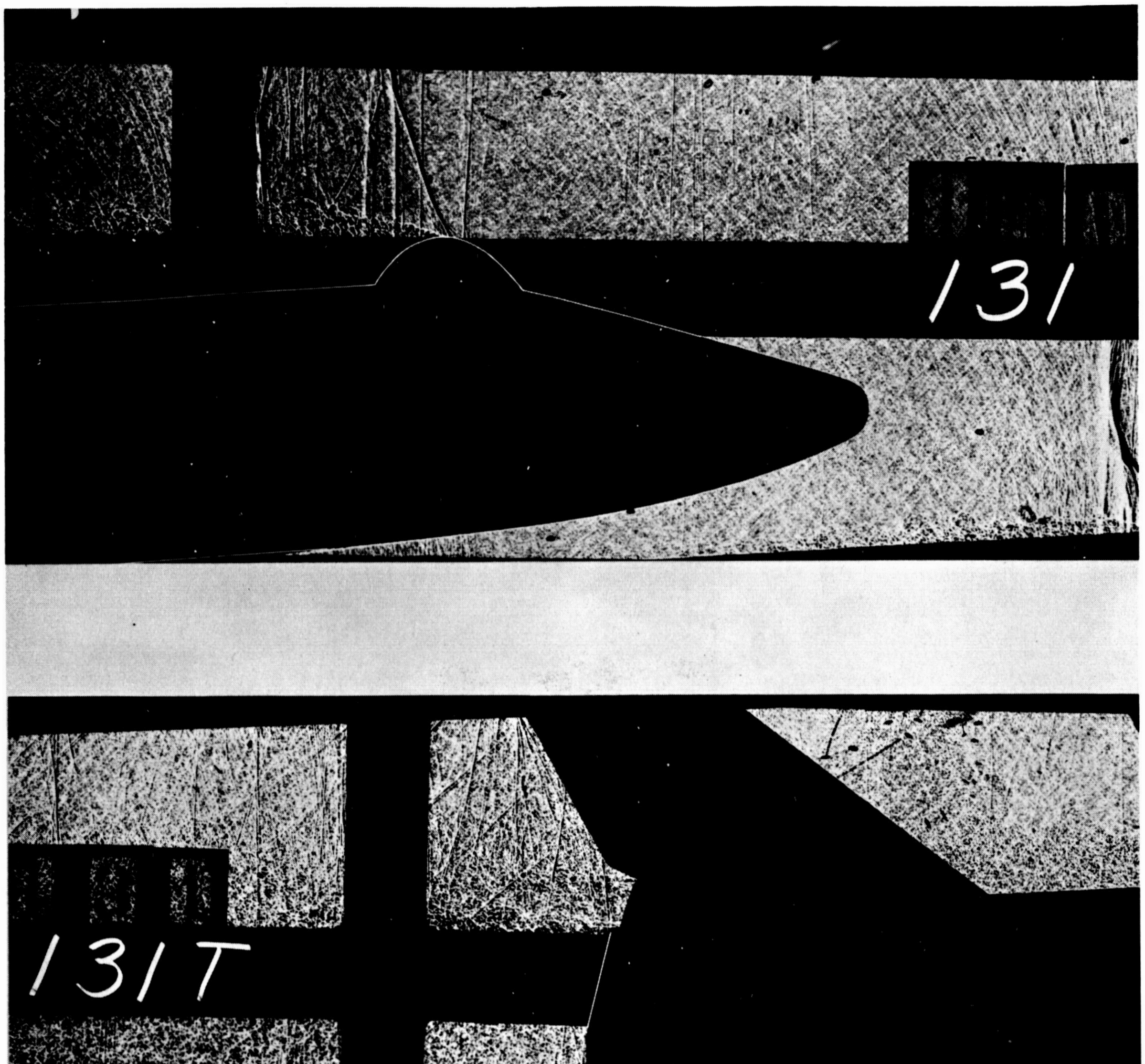

(c) $\alpha = 4°$, $\beta = 5°$, $q_{\infty} = 711$ psf

Figure 4. - Concluded.

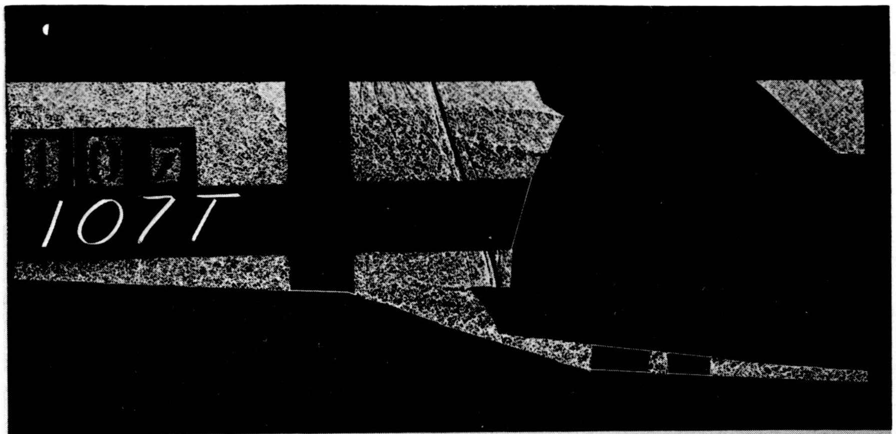

(a) $\alpha = -4°$, $\beta = 5°$, $q_\infty = 787$ psf

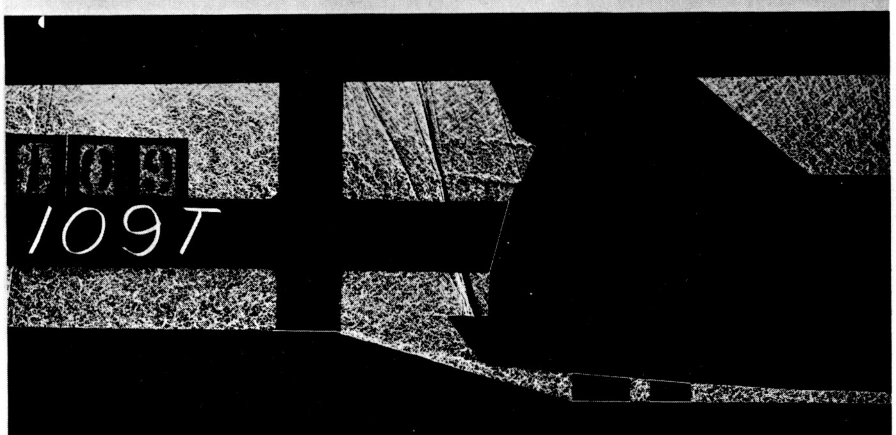

(b) $\alpha = 0°$, $\beta = 5°$, $q_\infty = 784$ psf

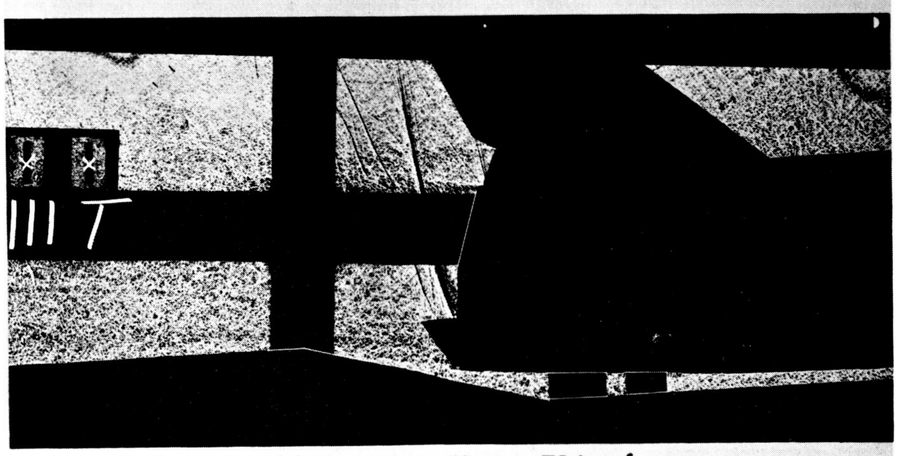

(c) $\alpha = 4°$, $\beta = 5°$, $q_\infty = 784$ psf

Figure 5. - Shadowgraphs of series-burn configuration 1 at $M_\infty = 1.00$.

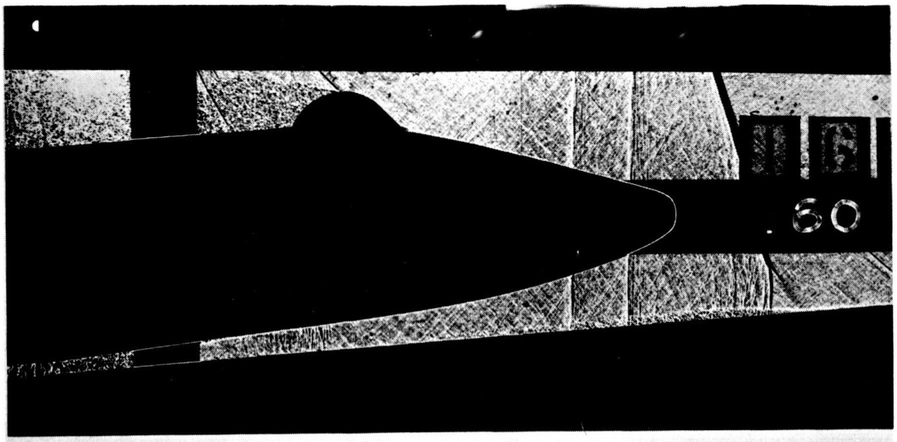

(d) $\alpha = 4°$, $\beta = 5°$, $q_{\infty} = 786$ psf

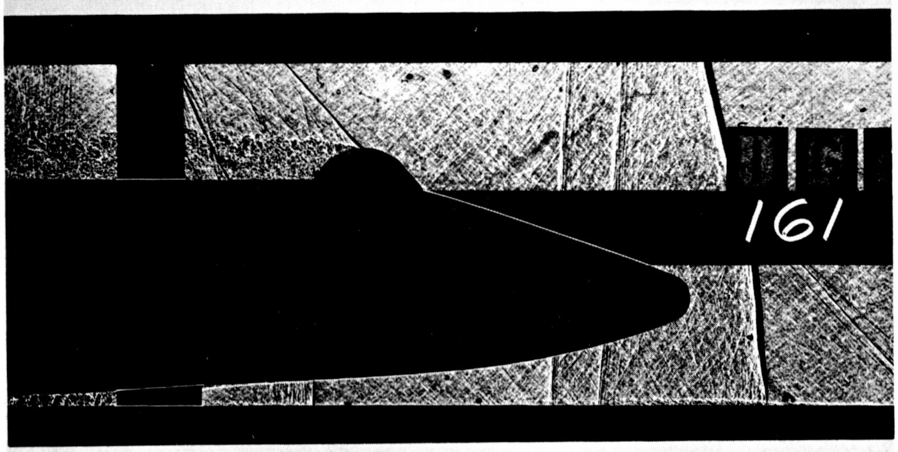

(e) $\alpha = 0°$, $\beta = 5°$, $q_{\infty} = 783$ psf

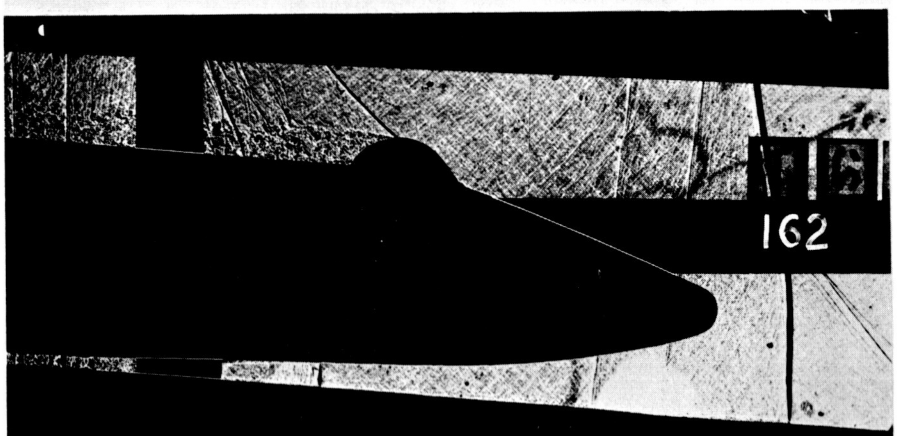

(f) $\alpha = -4°$, $\beta = 5°$, $q_{\infty} = 787$ psf

Figure 5. - Concluded.

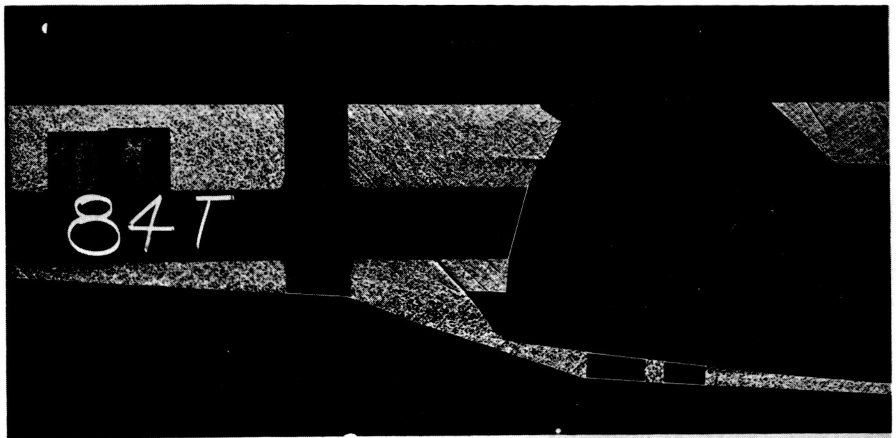

(a) $\alpha = -4°$, $\beta = 5°$, $q_{\infty} = 457$ psf

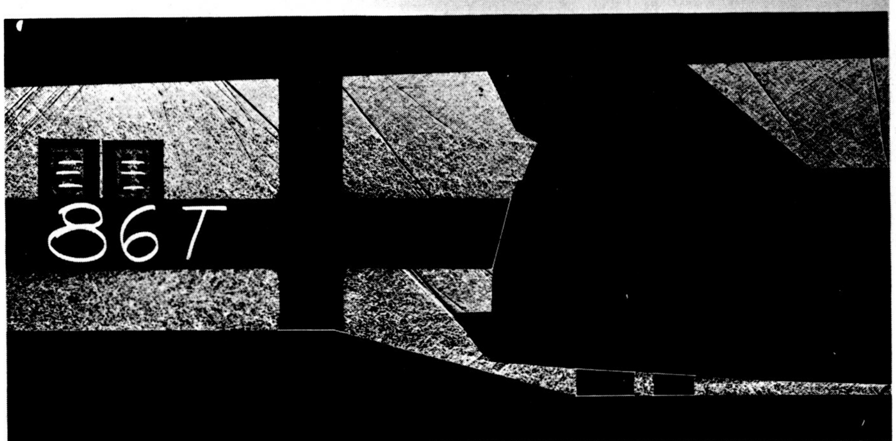

(b) $\alpha = 0°$, $\beta = 5°$, $q_{\infty} = 457$ psf

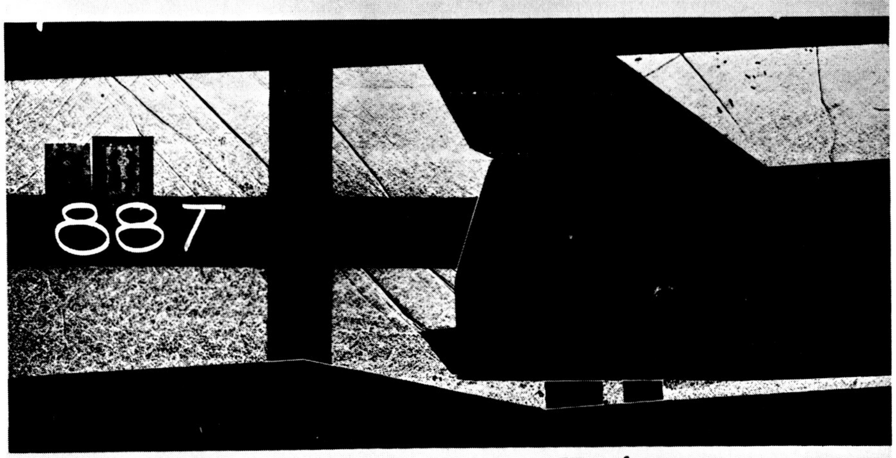

(c) $\alpha = 4°$, $\beta = 5°$, $q_{\infty} = 457$ psf

Figure 6. - Shadowgraphs of series-burn configuration 1 at $M_{\infty} = 1.40$.

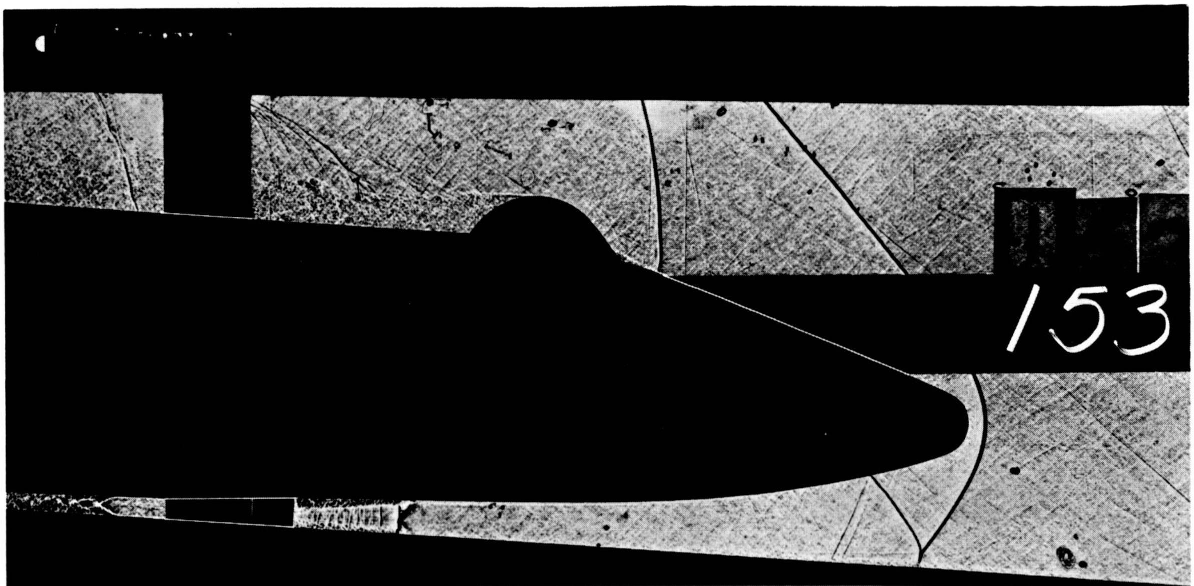

(d) $\alpha = -4°$, $\beta = 0°$, $q_\infty = 465$ psf

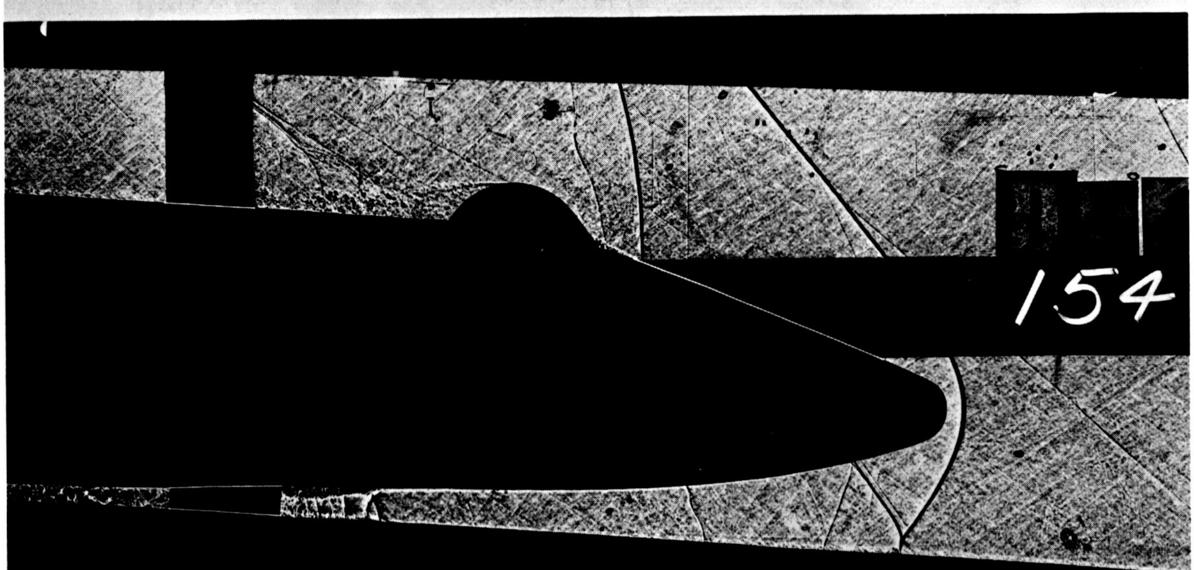

(e) $\alpha = -4°$, $\beta = 5°$, $q_\infty = 465$ psf

Figure 6. - Continued.

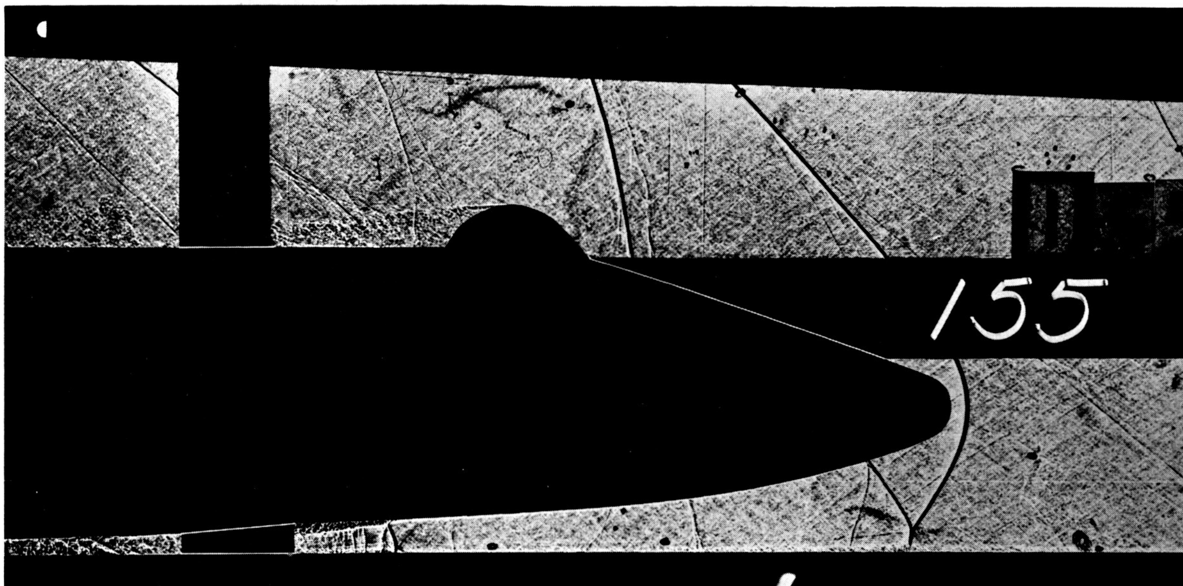

(f) $\alpha = 0°$, $\beta = 5°$, $q_{\infty} = 466$ psf

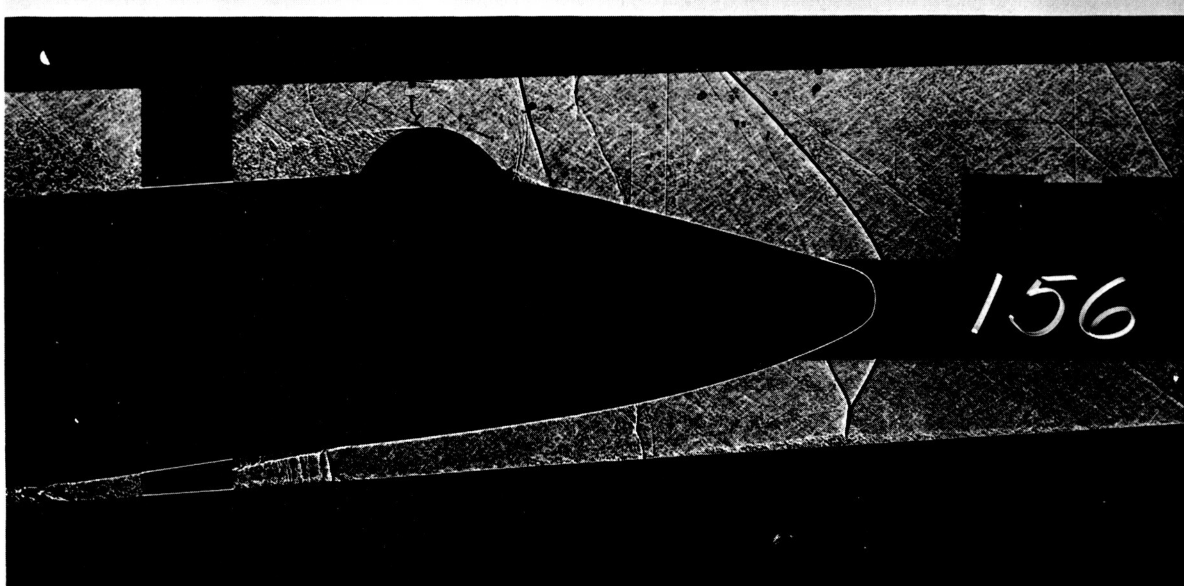

(g) $\alpha = 4°$, $\beta = 5°$, $q_{\infty} = 465$ psf

Figure 6. - Concluded.

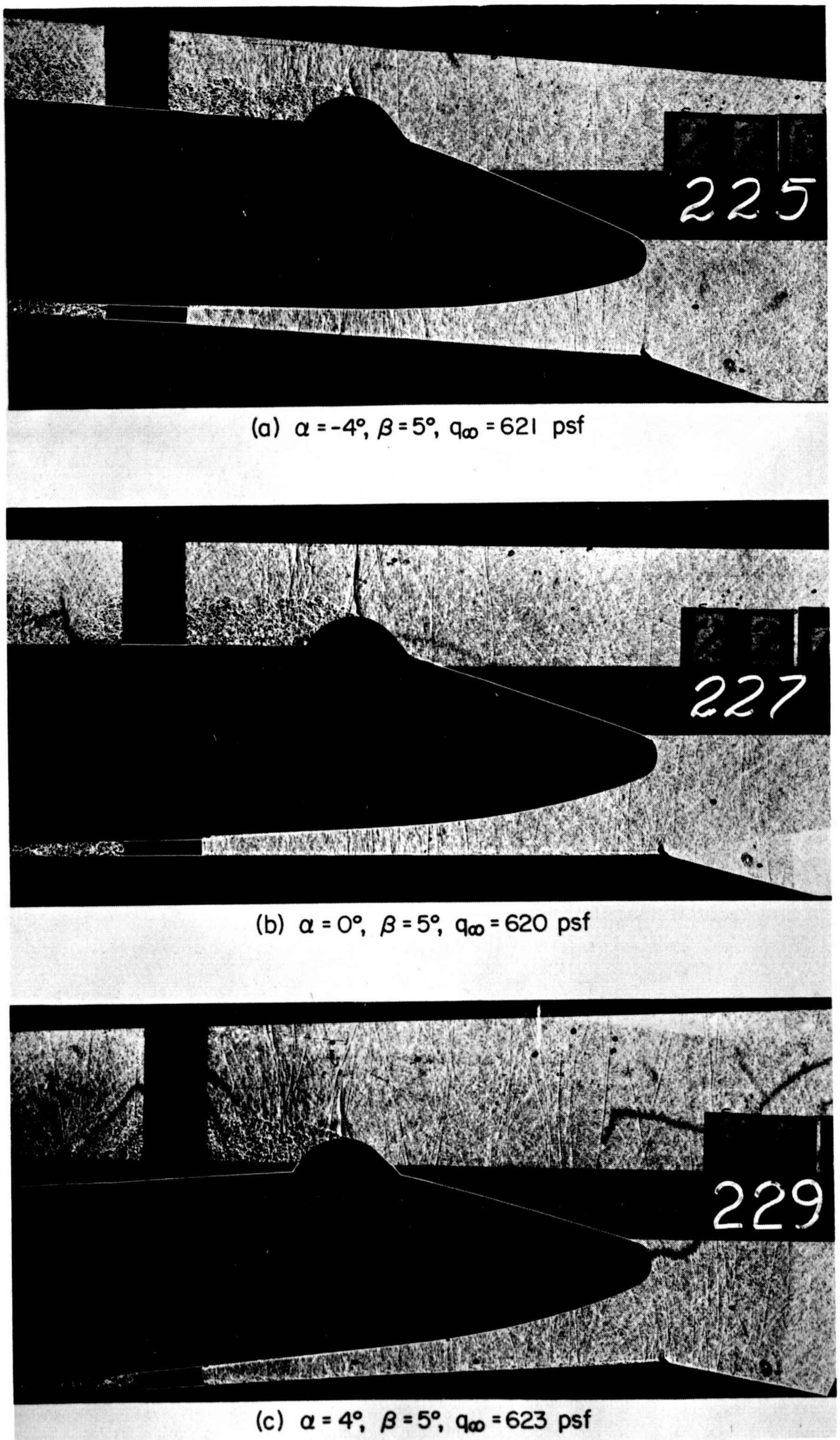

(a) $\alpha = -4°$, $\beta = 5°$, $q_\infty = 621$ psf

(b) $\alpha = 0°$, $\beta = 5°$, $q_\infty = 620$ psf

(c) $\alpha = 4°$, $\beta = 5°$, $q_\infty = 623$ psf

Figure 7. - Shadowgraphs of series-burn configuration 2 at $M_\infty = 0.80$.

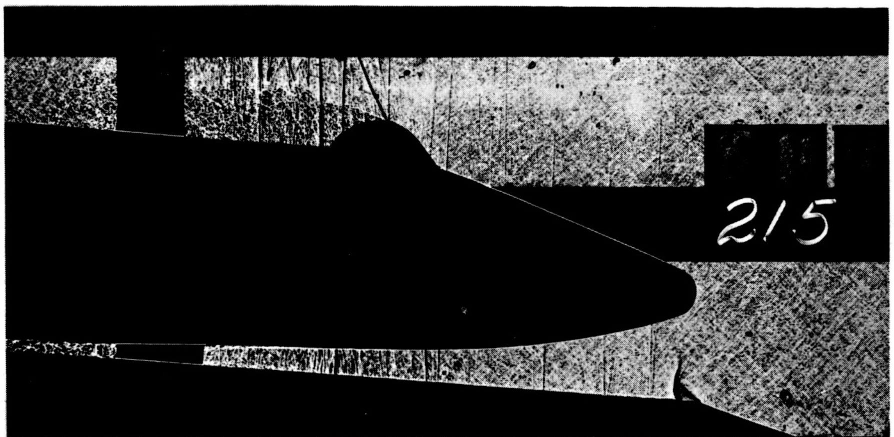

(a) $\alpha = -4°$, $\beta = 5°$, $q_\infty = 709$ psf

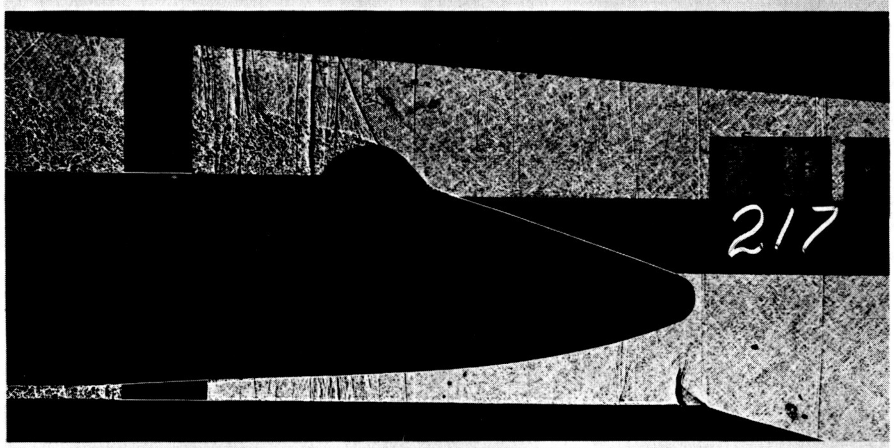

(b) $\alpha = 0°$, $\beta = 5°$, $q_\infty = 709$ psf

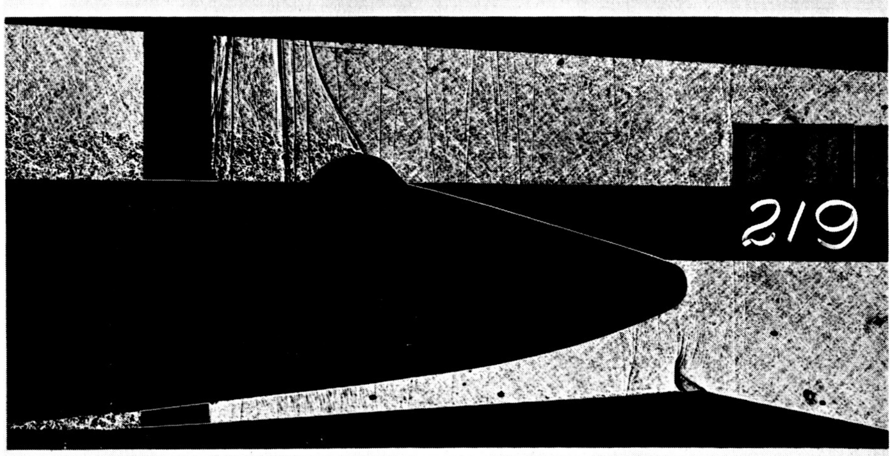

(c) $\alpha = 4°$, $\beta = 5°$, $q_\infty = 707$ psf

Figure 8. - Shadowgraphs of series-burn configuration 2 at $M_\infty = 0.90$.

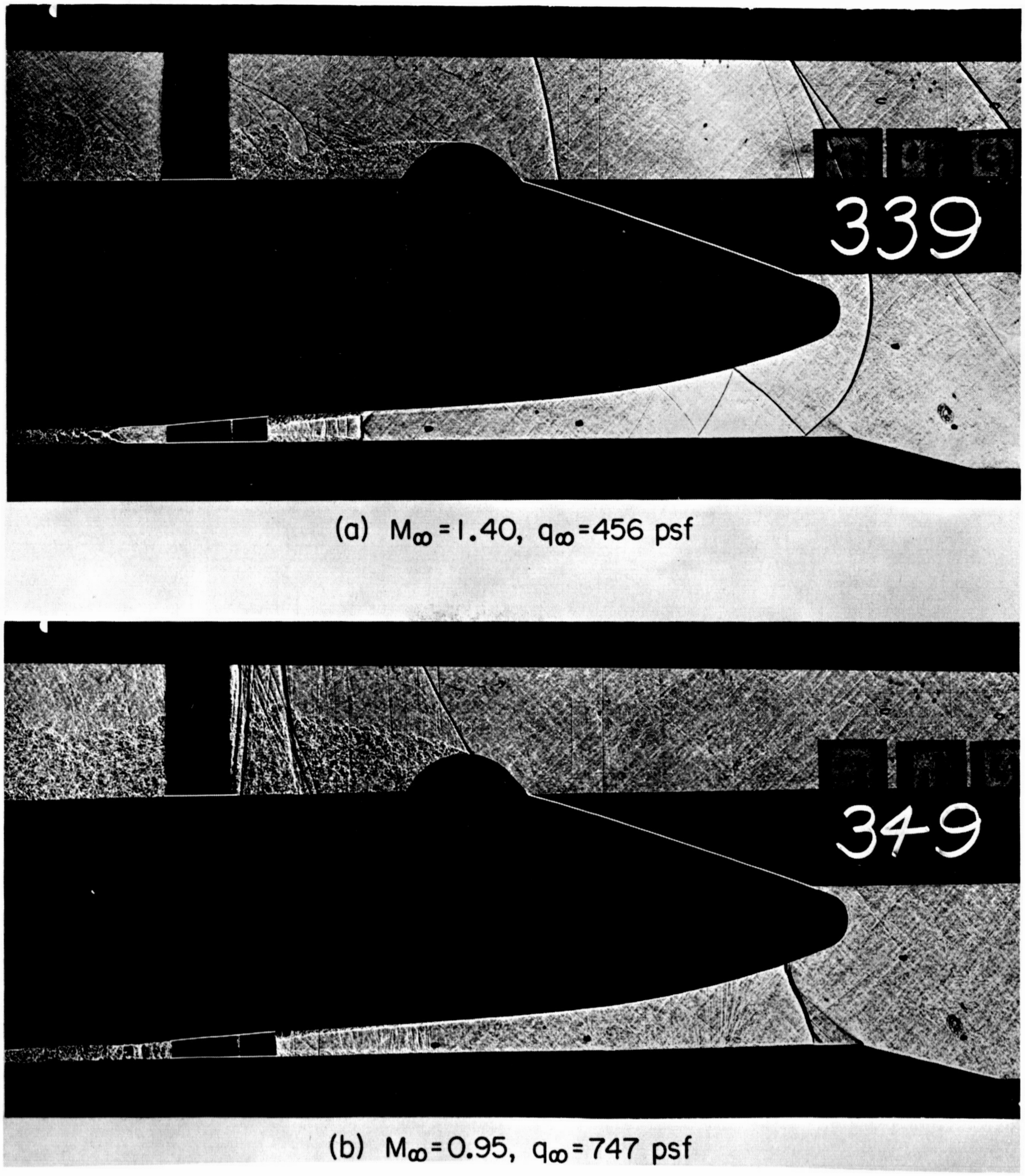

(a) $M_\infty = 1.40$, $q_\infty = 456$ psf

(b) $M_\infty = 0.95$, $q_\infty = 747$ psf

Figure 9. - Shadowgraphs of series-burn configuration 2 with both angle of attack and angle of sideslip equal to 0°.

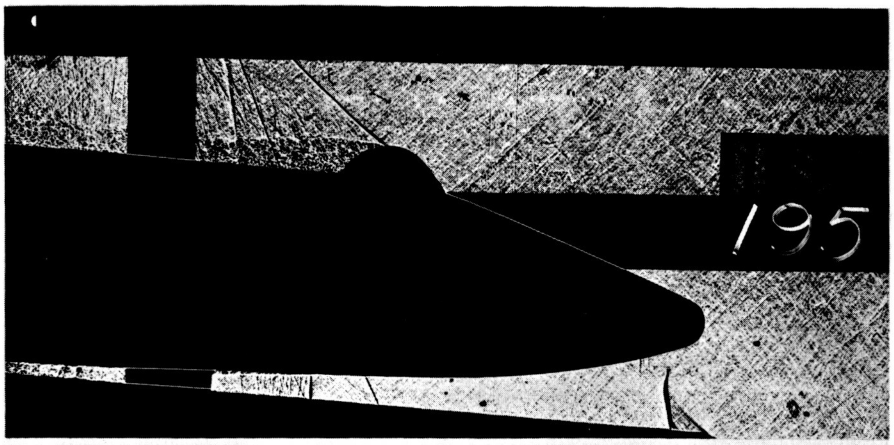

(a) $\alpha = -4°$, $\beta = 5°$, $q_\infty = 786$ psf

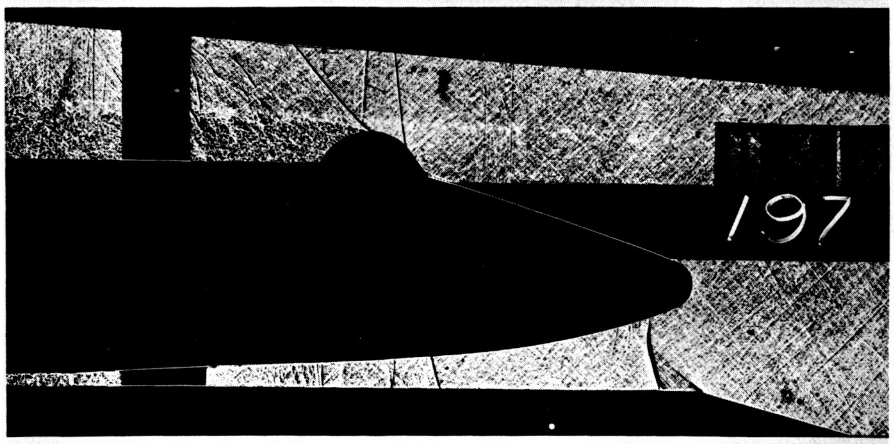

(b) $\alpha = 0°$, $\beta = 5°$, $q_\infty = 783$ psf

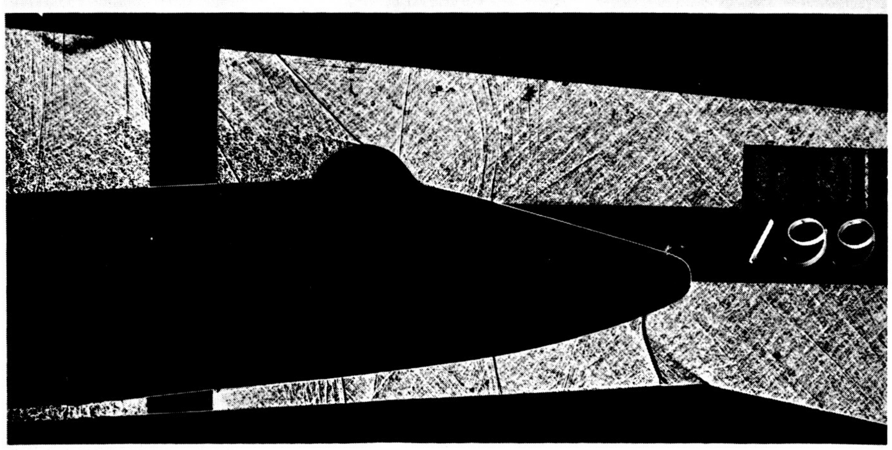

(c) $\alpha = 4°$, $\beta = 5°$, $q_\infty = 786$ psf

Figure 10. - Shadowgraphs of series-burn configuration 2 at $M_\infty = 1.00$.

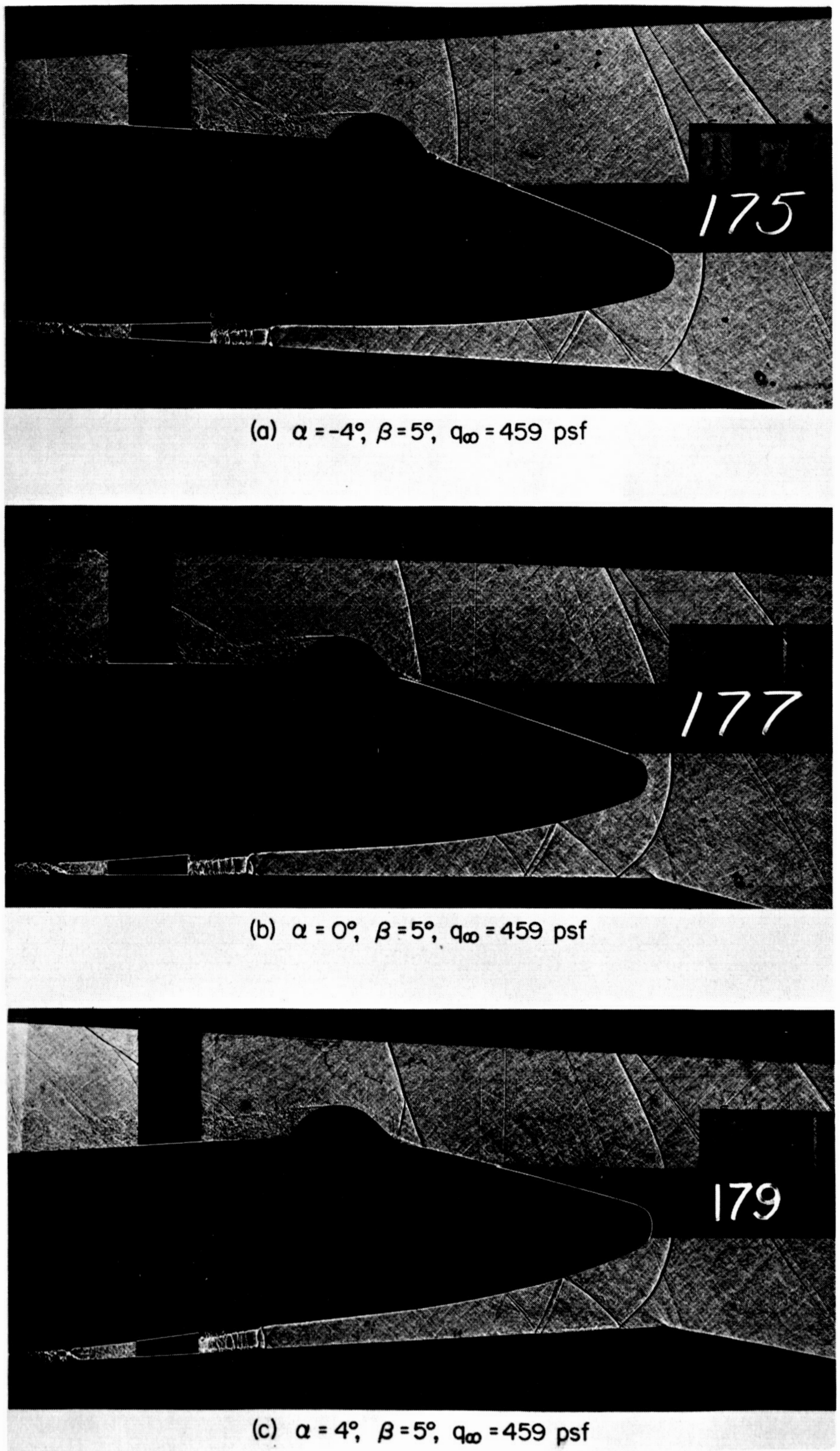

(a) $\alpha = -4°$, $\beta = 5°$, $q_\infty = 459$ psf

(b) $\alpha = 0°$, $\beta = 5°$, $q_\infty = 459$ psf

(c) $\alpha = 4°$, $\beta = 5°$, $q_\infty = 459$ psf

Figure 11. - Shadowgraphs of series-burn configuration 2 at M_∞ = 1.40.

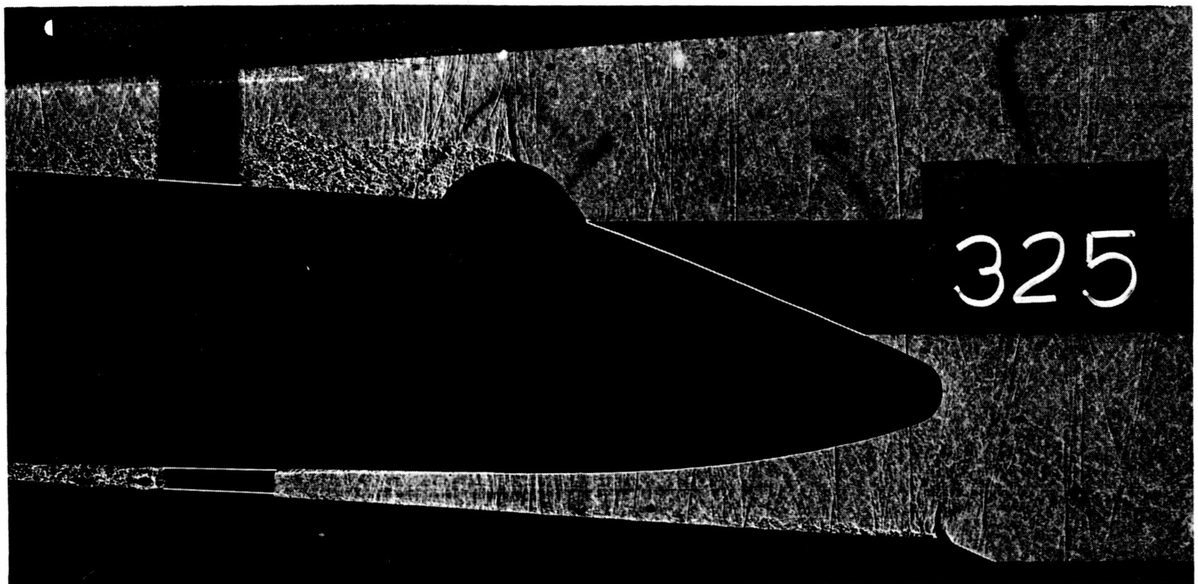

(a) $\alpha = -4°$, $\beta = 5°$, $q_{\infty} = 622$ psf

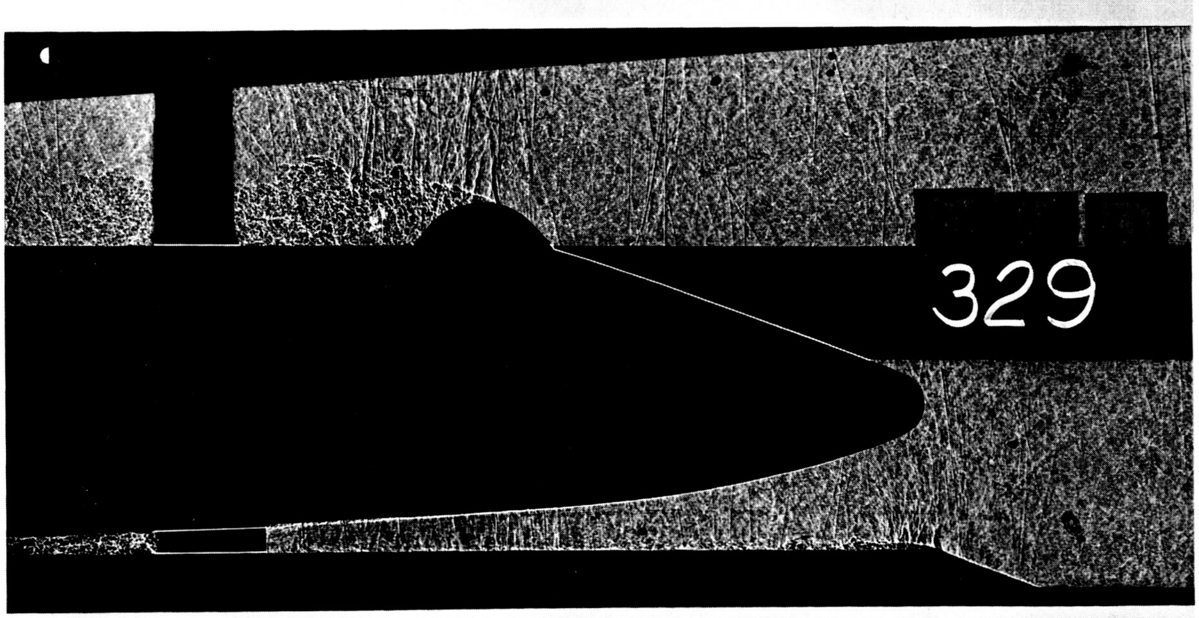

(b) $\alpha = 0°$, $\beta = 5°$, $q_{\infty} = 619$ psf

Figure 12. - Shadowgraphs of series-burn configuration 3 at $M_{\infty} = 0.80$.

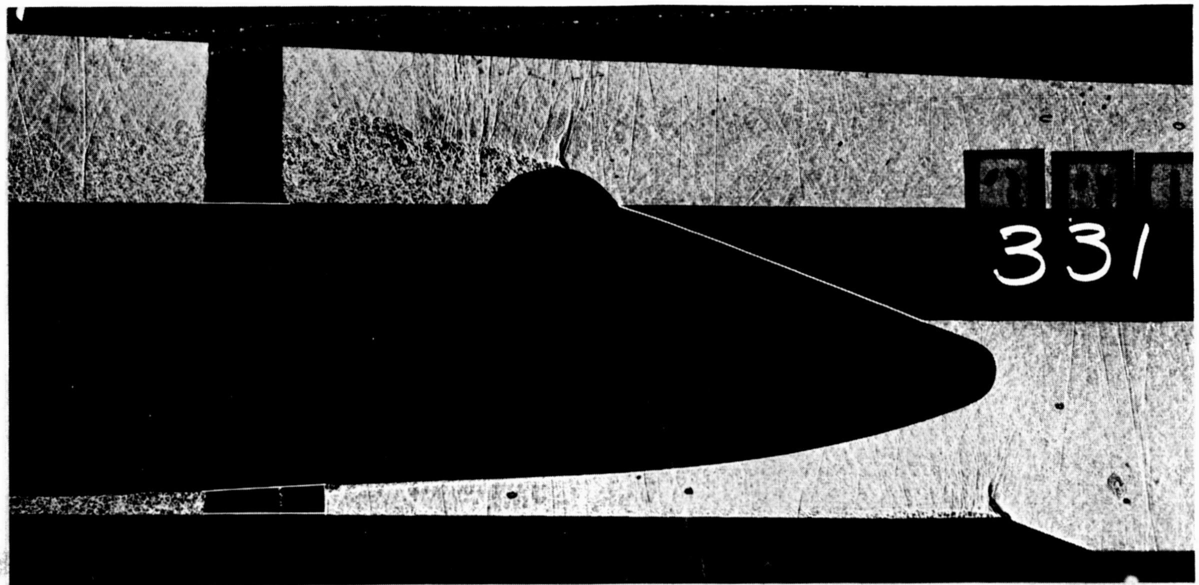

(c) $\alpha = 0°$, $\beta = 0°$, $q_{\infty} = 620$ psf

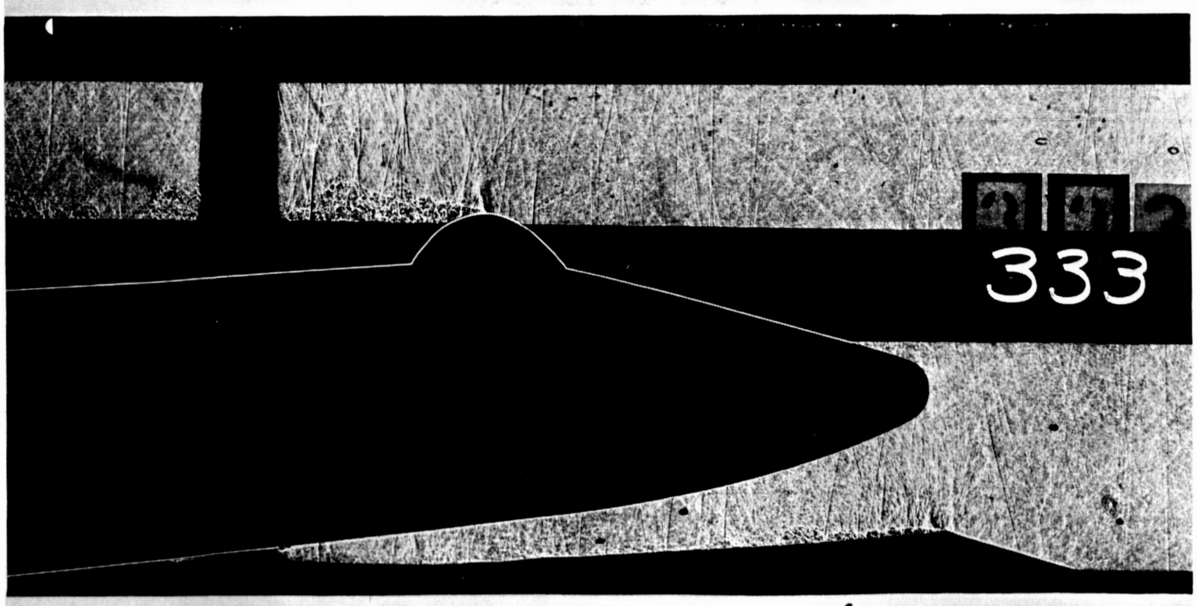

(d) $\alpha = 4°$, $\beta = 0°$, $q_{\infty} = 621$ psf

Figure 12. - Concluded.

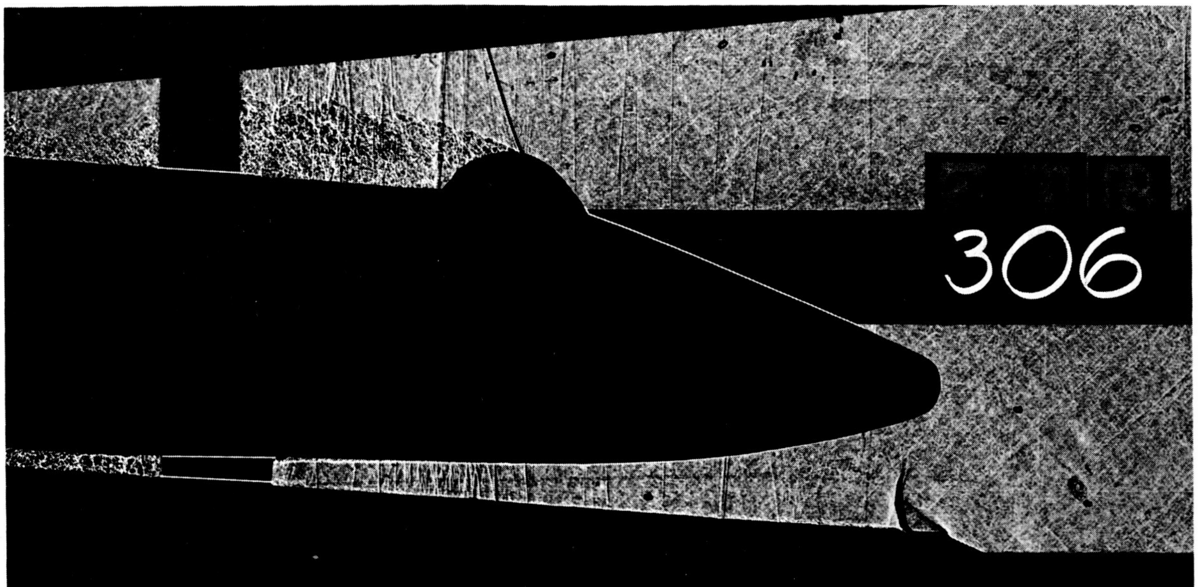

(a) $\alpha = -4°$, $\beta = 5°$, $q_{\infty} = 711$ psf

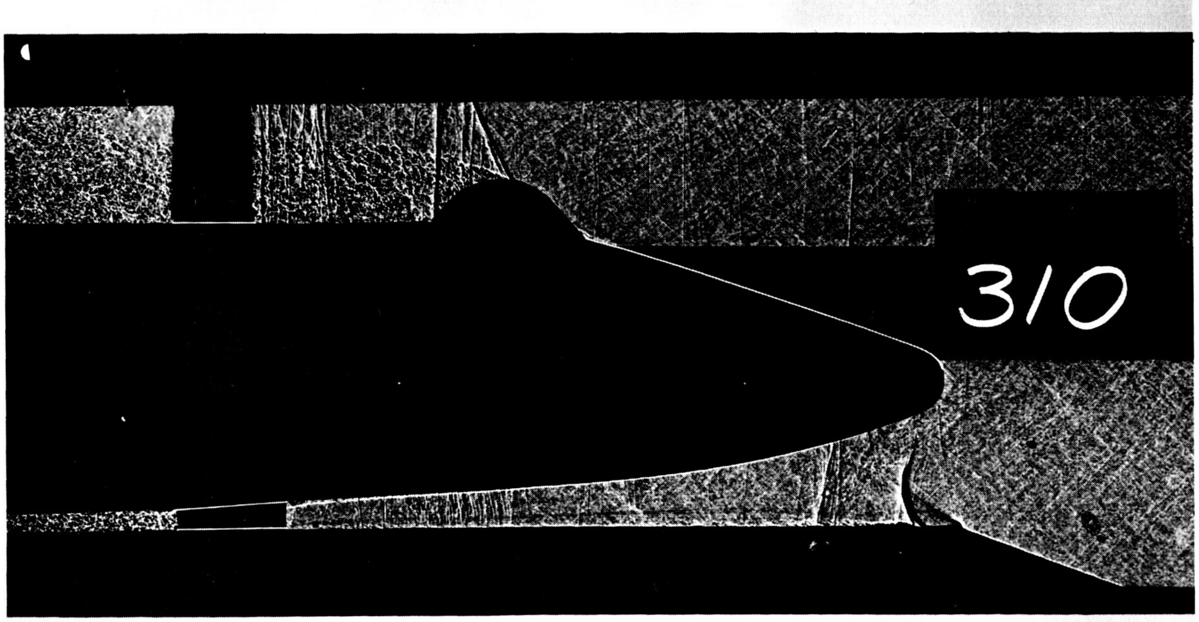

(b) $\alpha = 0°$, $\beta = 5°$, $q_{\infty} = 709$ psf

Figure 13. - Shadowgraphs of series-burn configuration 3 at $M_{\infty} = 0.90$.

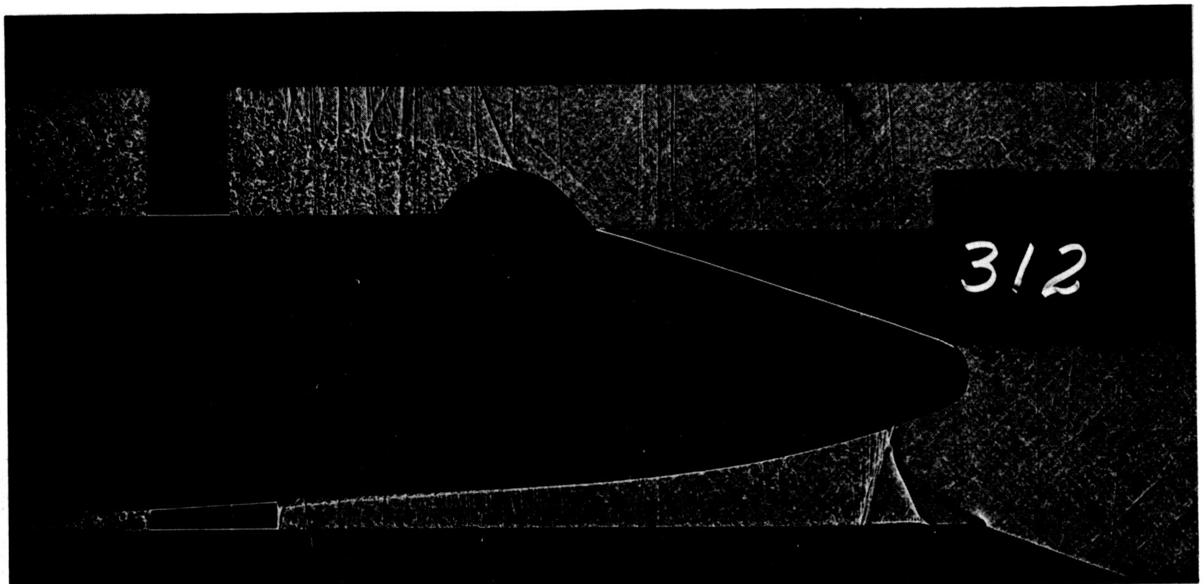

(c) $\alpha = 0°$, $\beta = 0°$, $q_{\infty} = 711$ psf

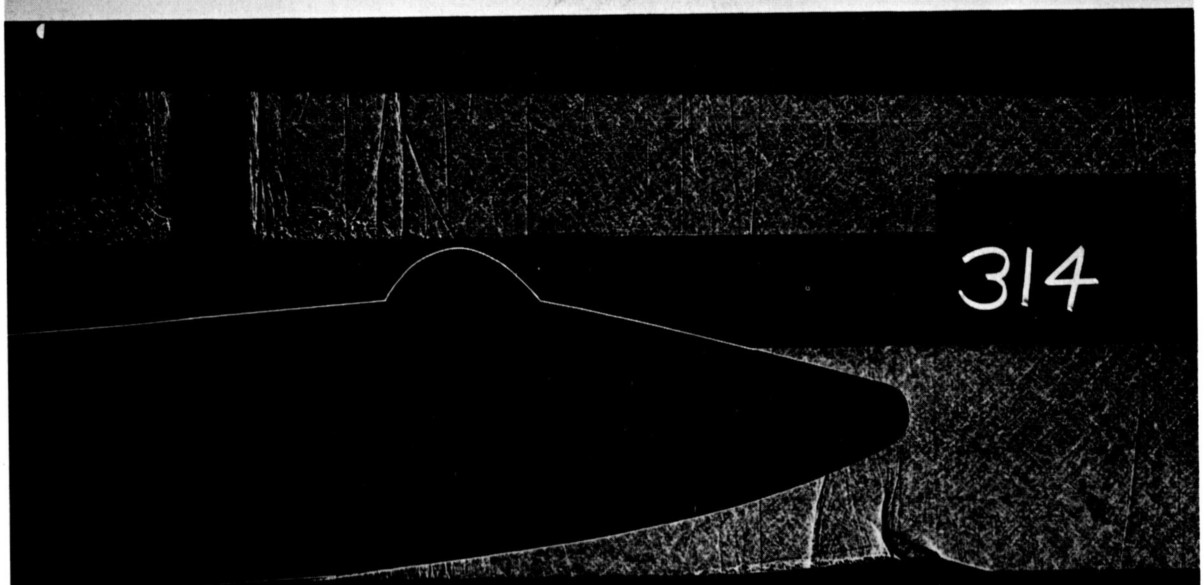

(d) $\alpha = 4°$, $\beta = 5°$, $q_{\infty} = 711$ psf

Figure 13 - Concluded.

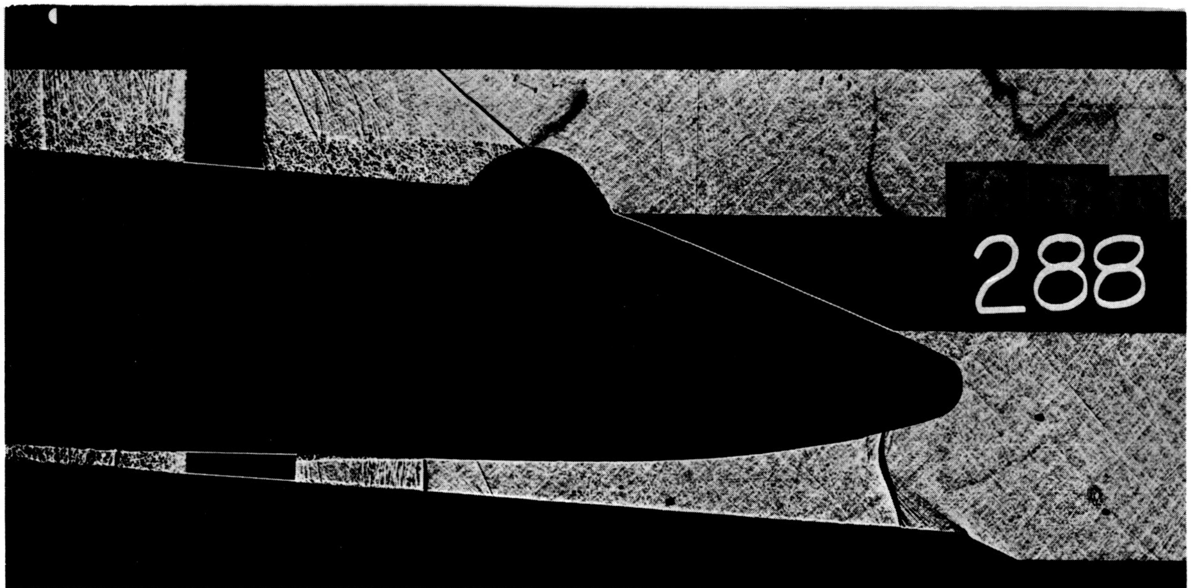

(a) $\alpha = -4°$, $\beta = 5°$, $q_{\infty} = 785$ psf

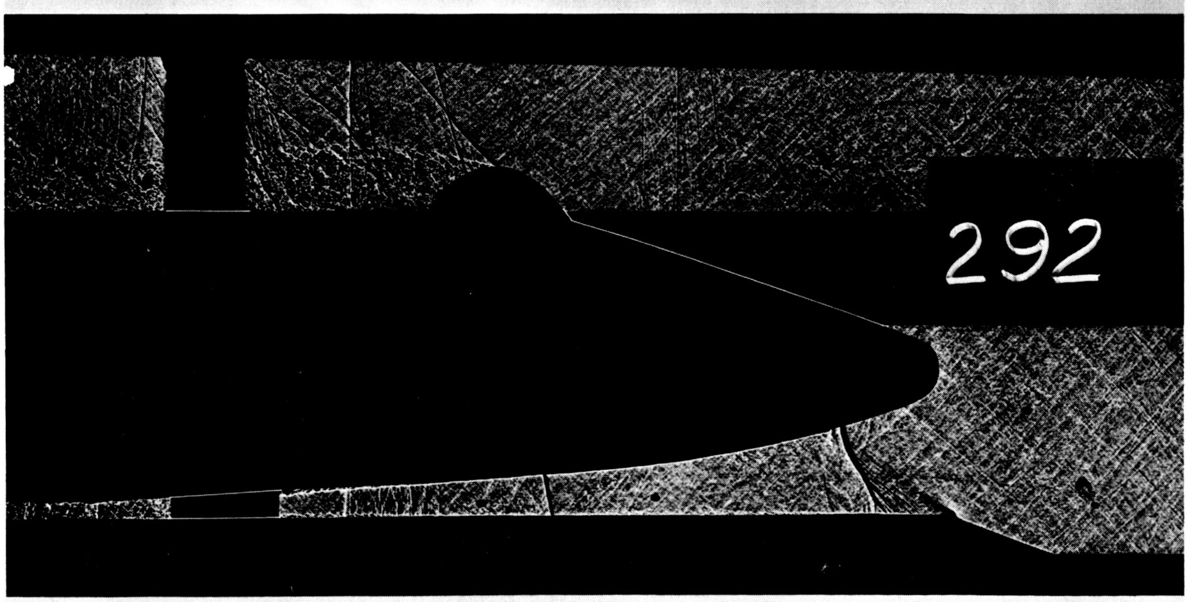

(b) $\alpha = 0°$, $\beta = 5°$, $q_{\infty} = 783$ psf

Figure 14. - Shadowgraphs of series-burn configuration 3 at $M_{\infty} = 1.00$.

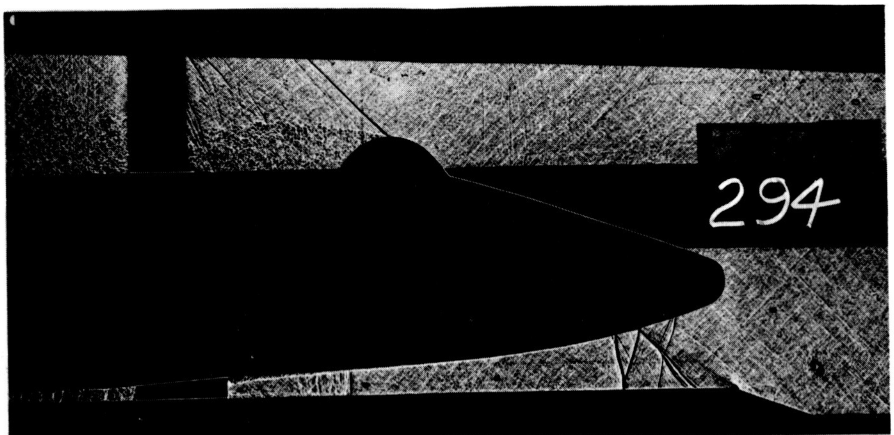

(c) $\alpha = 0°$, $\beta = 0°$, $q_\infty = 784$ psf

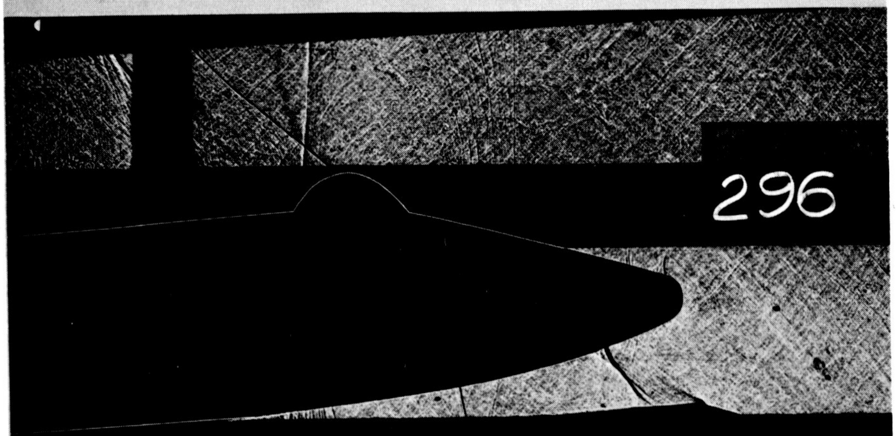

(d) $\alpha = 4°$, $\beta = 0°$, $q_\infty = 788$ psf

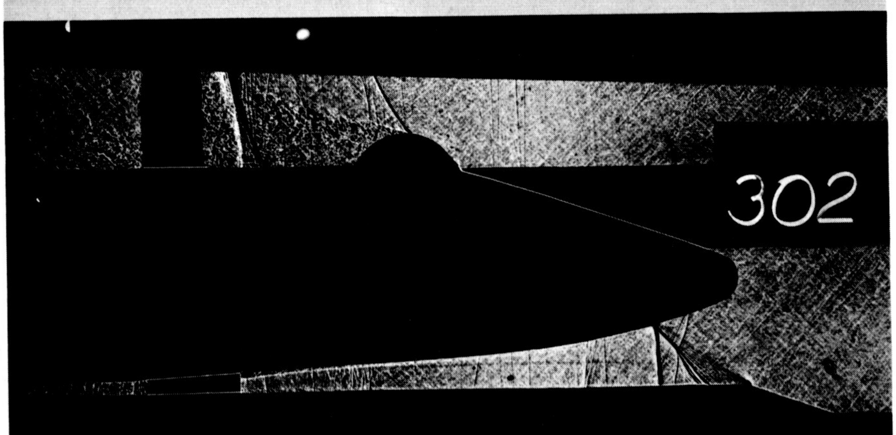

(e) $\alpha = 0°$, $\beta = 0°$, $q_\infty = 751$ psf

Figure 14. - Concluded.

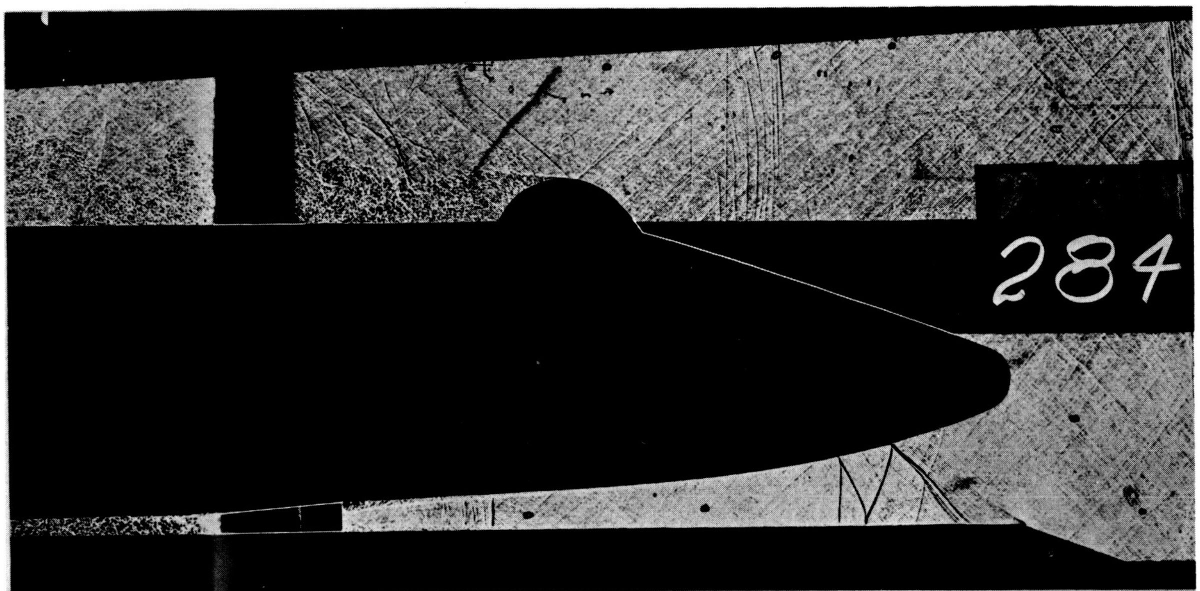

(a) $M_\infty = 1.10$, $q_\infty = 560$ psf

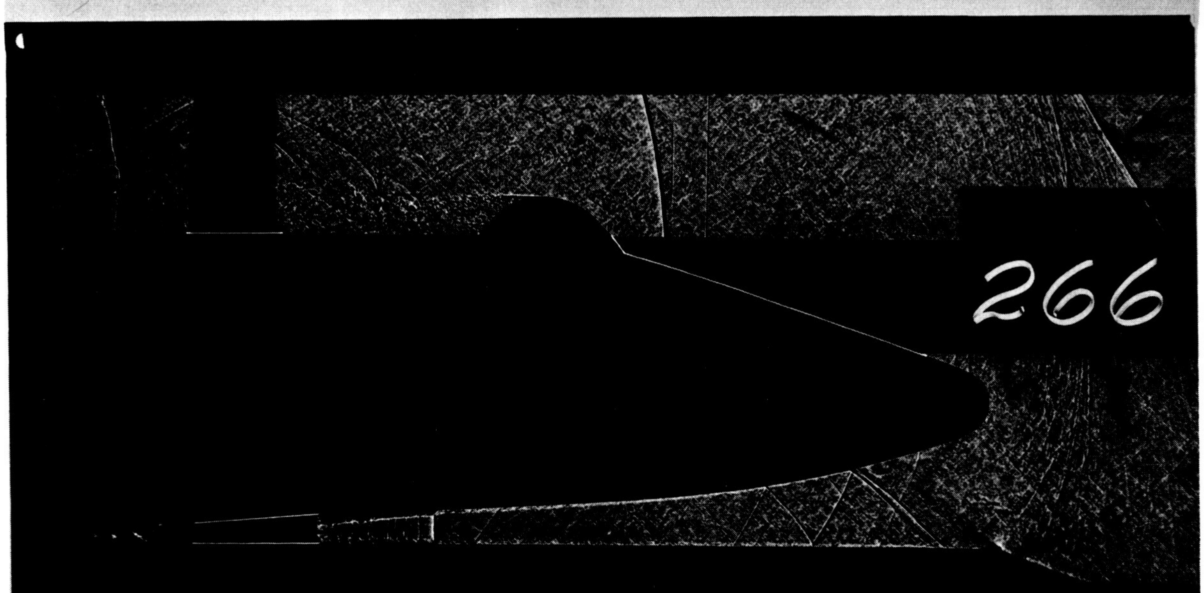

(b) $M_\infty = 1.30$, $q_\infty = 454$ psf

Figure 15. - Shadowgraphs of series-burn configuration 3 with both angle of attack and angle of sideslip equal to 0°.

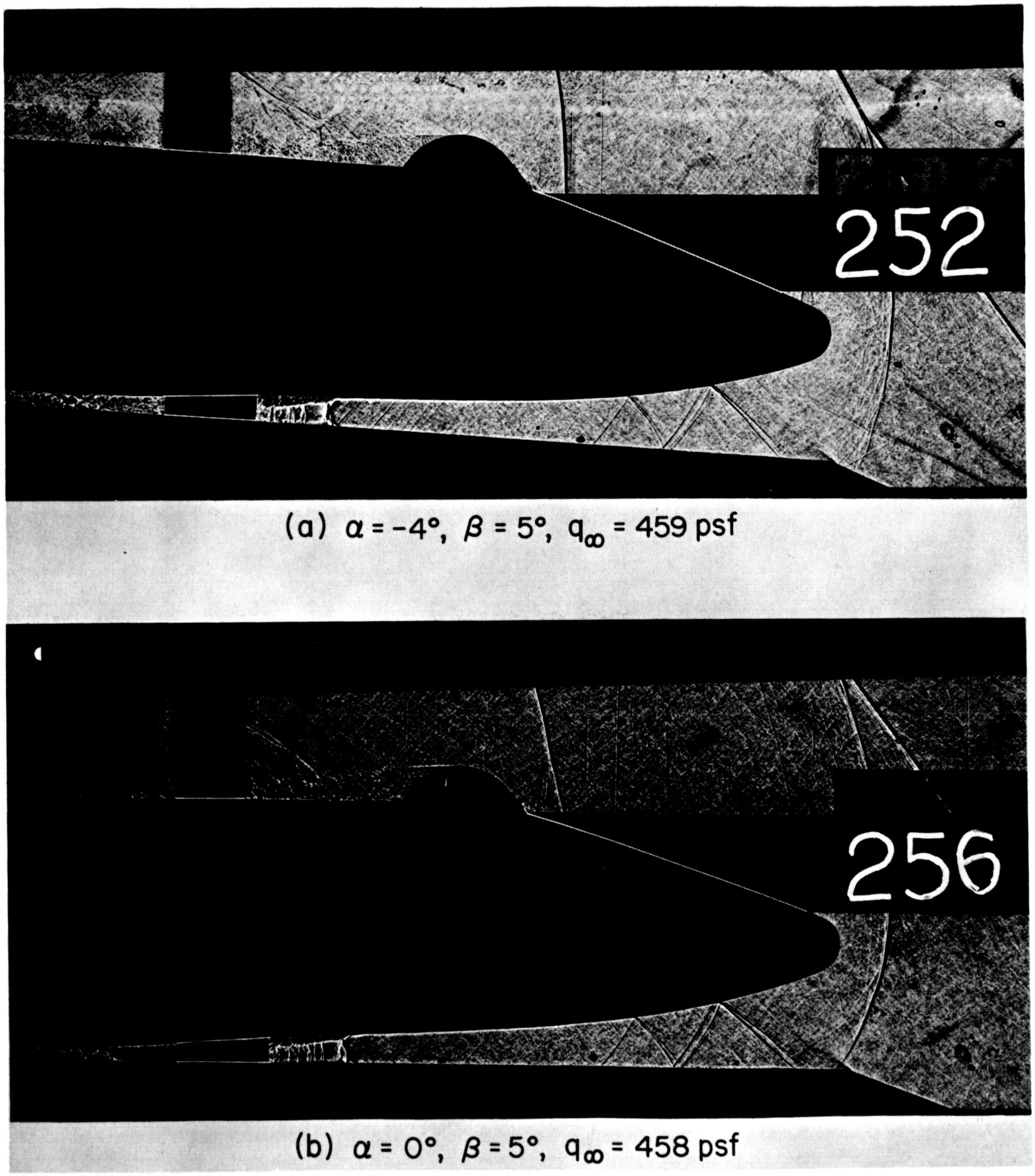

(a) $\alpha = -4°$, $\beta = 5°$, $q_\infty = 459$ psf

(b) $\alpha = 0°$, $\beta = 5°$, $q_\infty = 458$ psf

Figure 16. - Shadowgraphs of series-burn configuration 3 at $M_\infty = 1.39$.

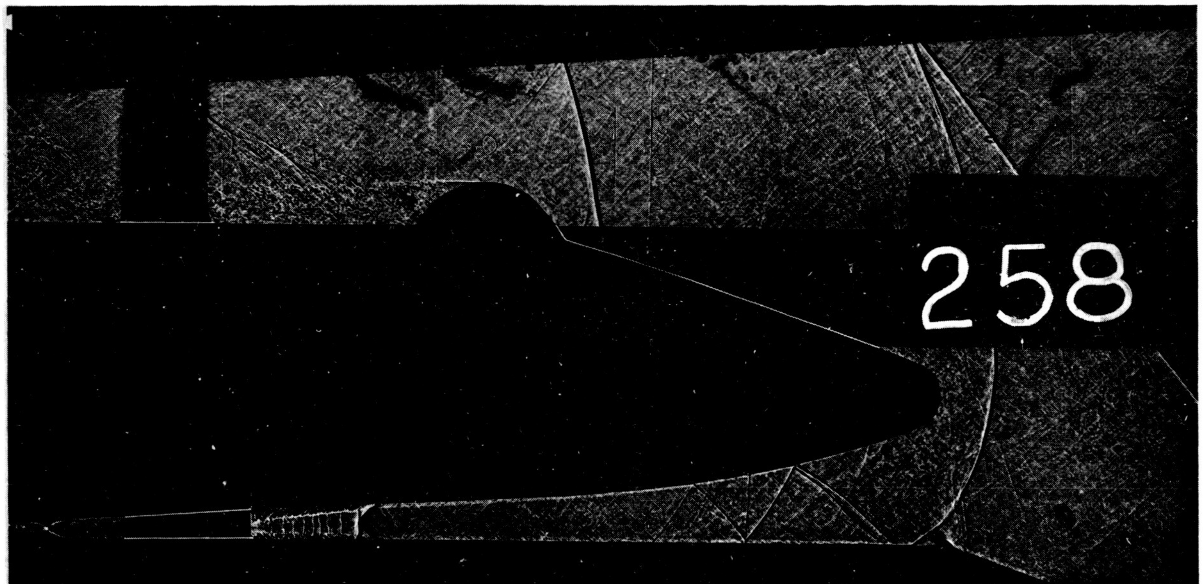

(a) $\alpha = 0°$, $\beta = 0°$, $q_\infty = 459$ psf

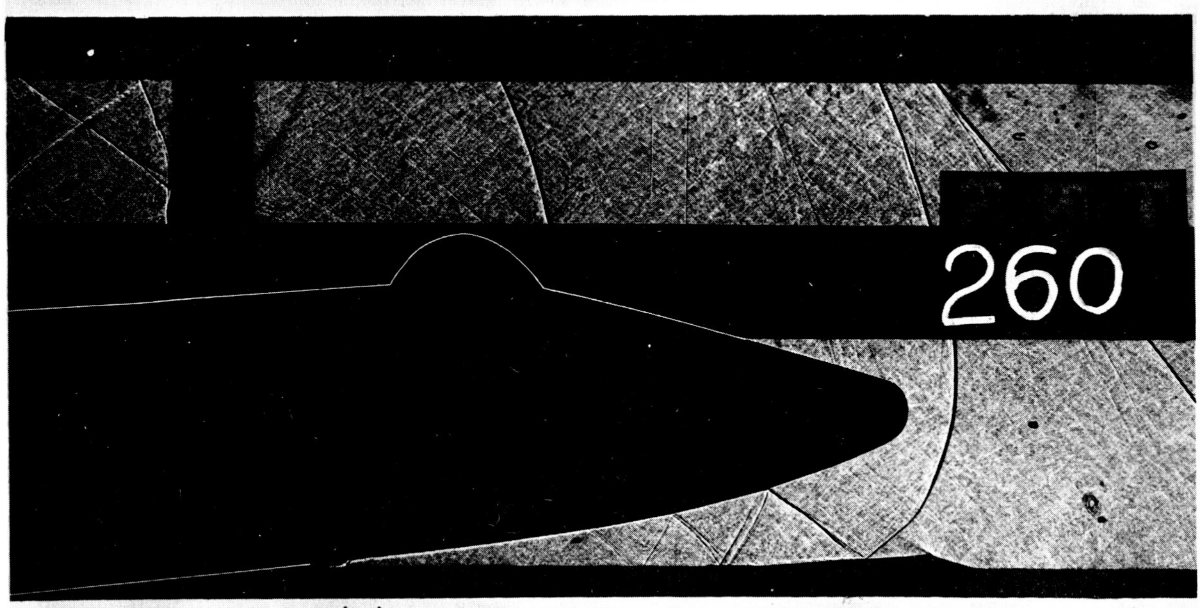

(b) $\alpha = 4°$, $\beta = 5°$, $q_\infty = 458$ psf

Figure 17. - Shadowgraphs of series-burn configuration 3 at $M_\infty = 1.40$.

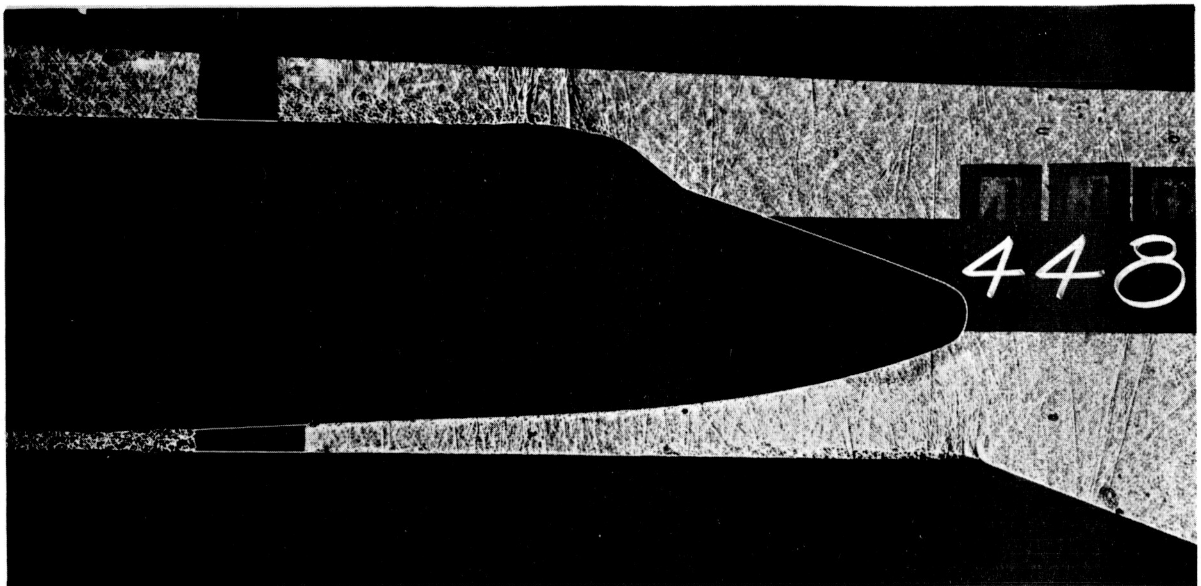

(a) $\alpha = 0°$, $\beta = 5°$, $q_\infty = 622$ psf

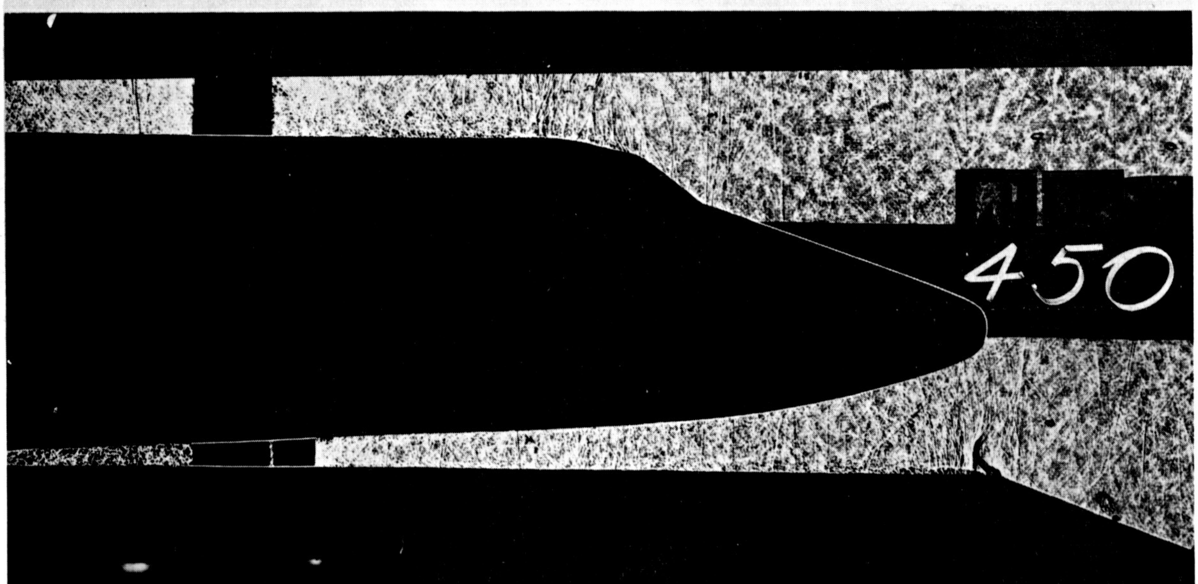

(b) $\alpha = 0°$, $\beta = 0°$, $q_\infty = 623$ psf

Figure 18. - Shadowgraphs of series-burn configuration 4 at $M_\infty = 0.80$.

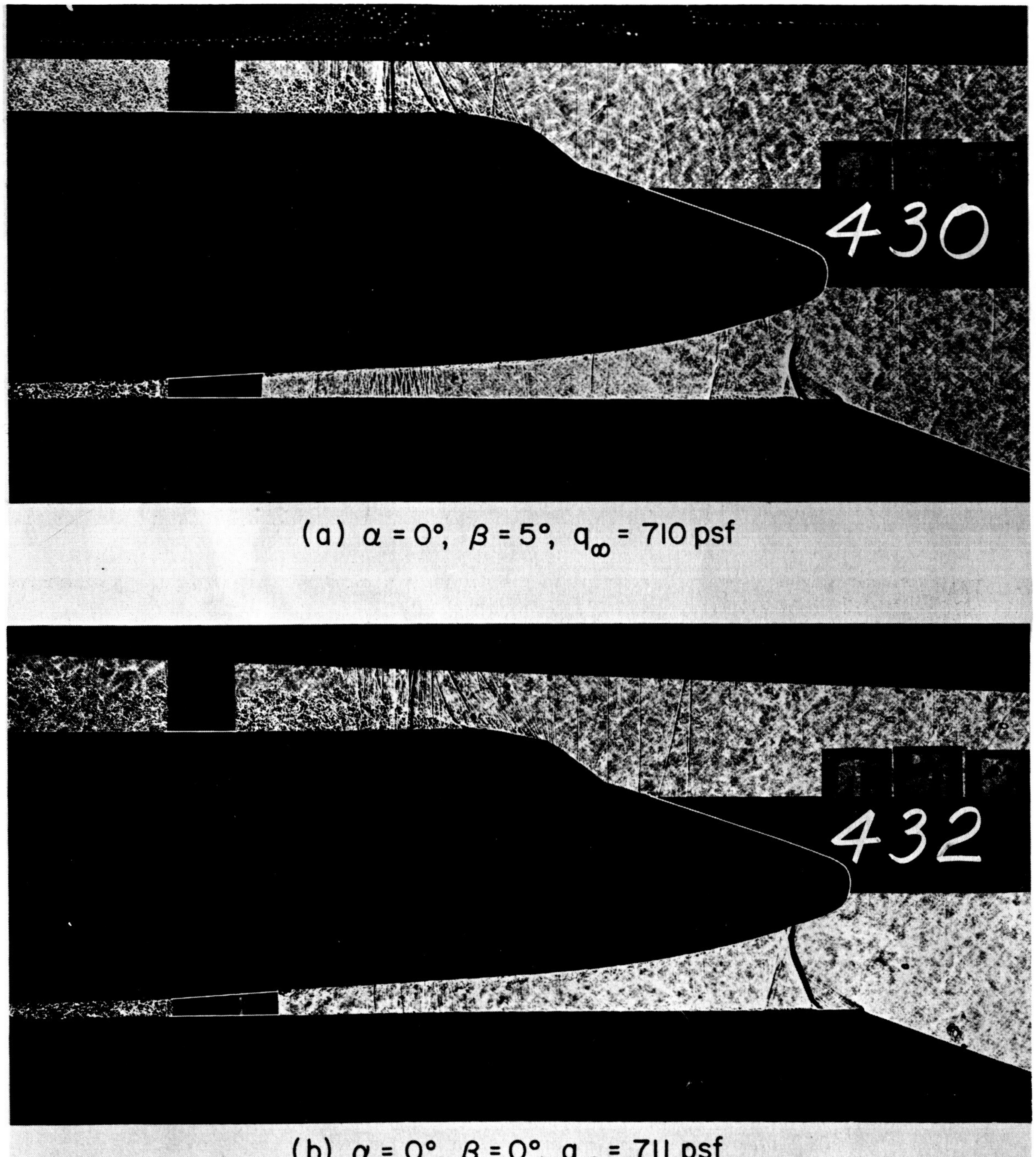

(a) $\alpha = 0°$, $\beta = 5°$, $q_{\infty} = 710$ psf

(b) $\alpha = 0°$, $\beta = 0°$, $q_{\infty} = 711$ psf

Figure 19. - Shadowgraphs of series-burn configuration 4 at $M_{\infty} = 0.90$.

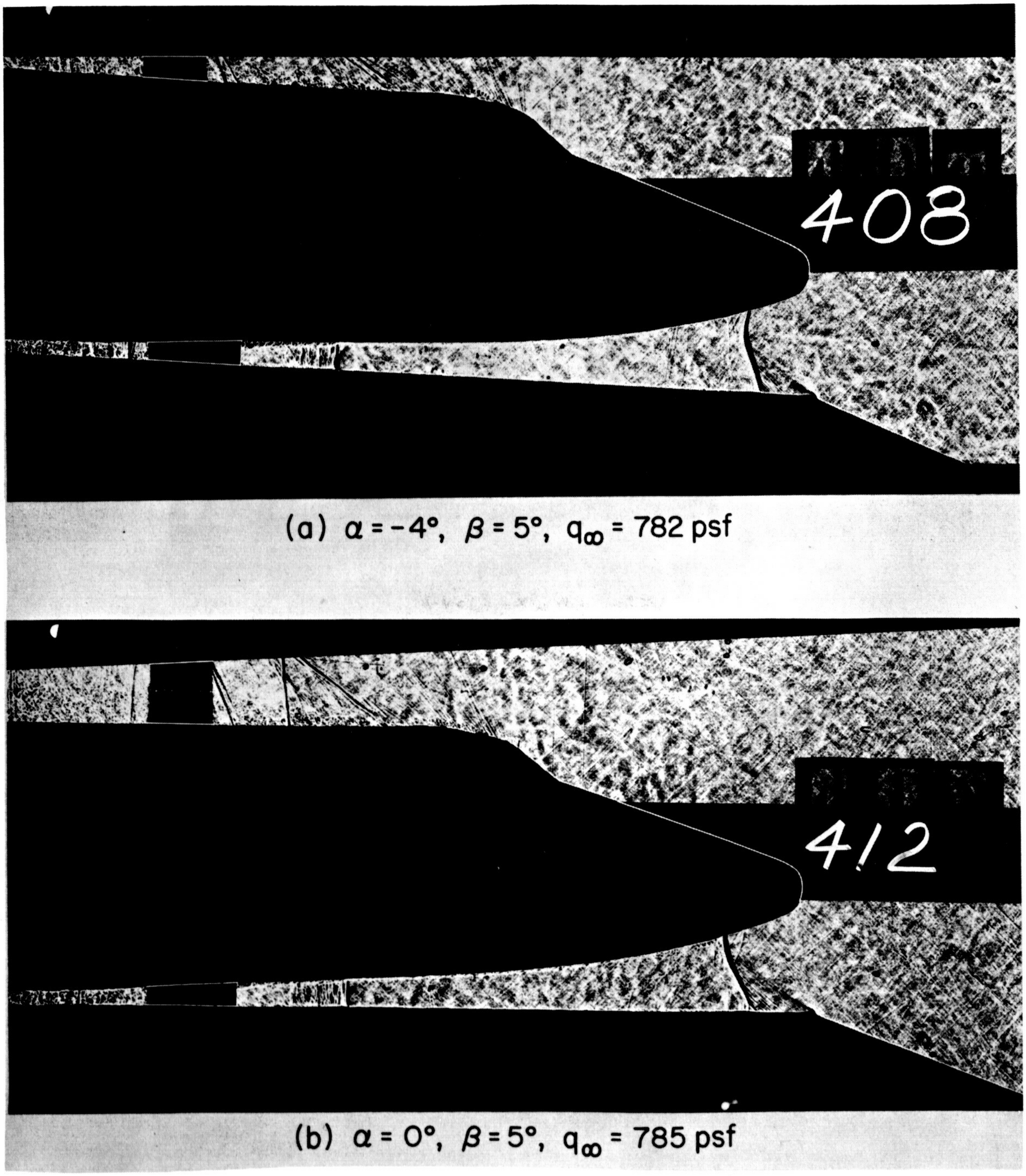

(a) $\alpha = -4°$, $\beta = 5°$, $q_\infty = 782$ psf

(b) $\alpha = 0°$, $\beta = 5°$, $q_\infty = 785$ psf

Figure 20. - Shadowgraphs of series-burn configuration 4 at $M_\infty = 1.00$.

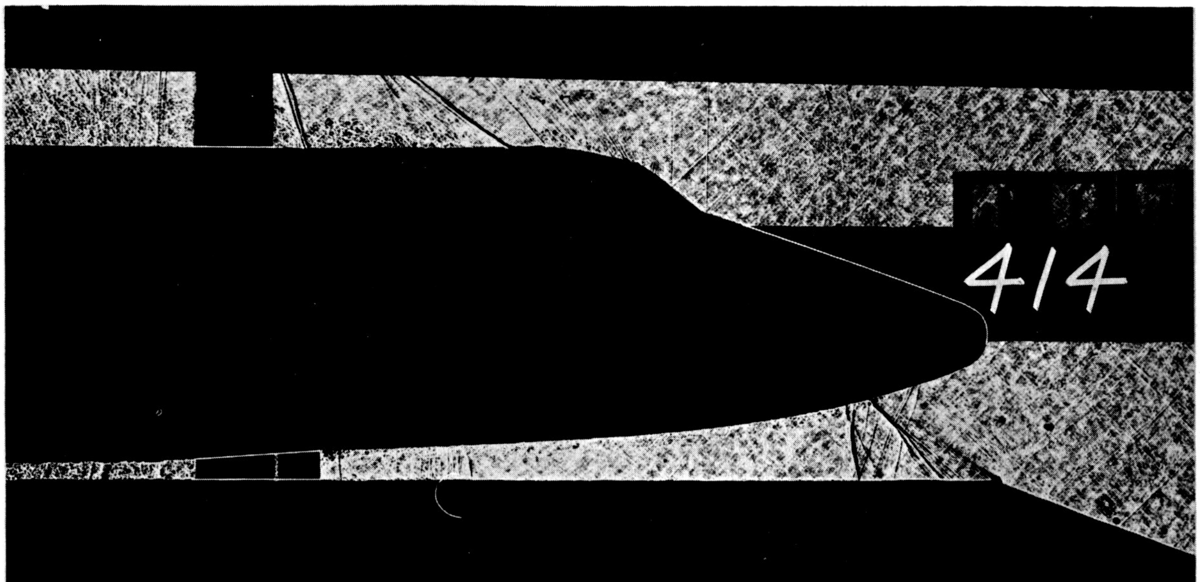

(c) $\alpha = 0°$, $\beta = 0°$, $q_\infty = 787$ psf

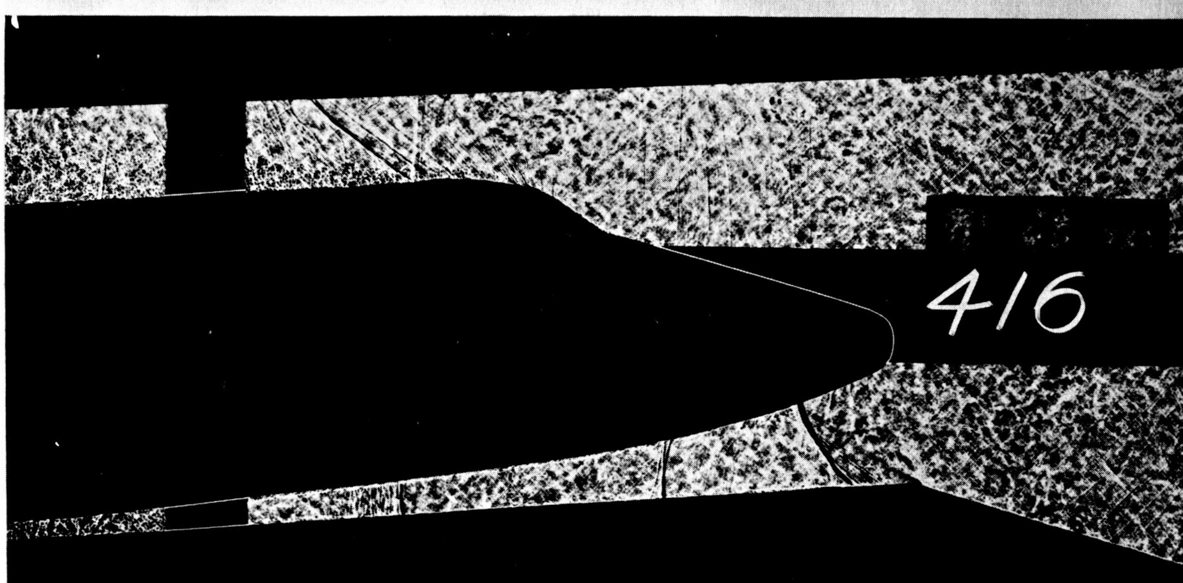

(d) $\alpha = 4°$, $\beta = 5°$, $q_\infty = 786$ psf

Figure 20. - Concluded.

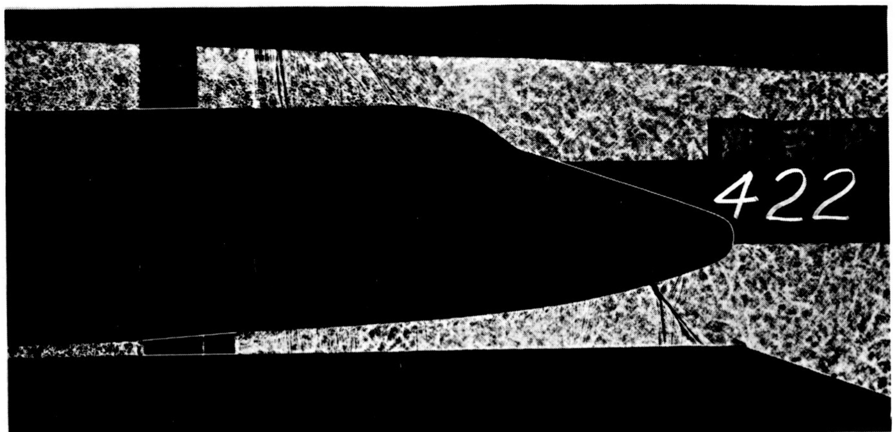

(a) $M_\infty = 0.95$, $q_\infty = 751$ psf

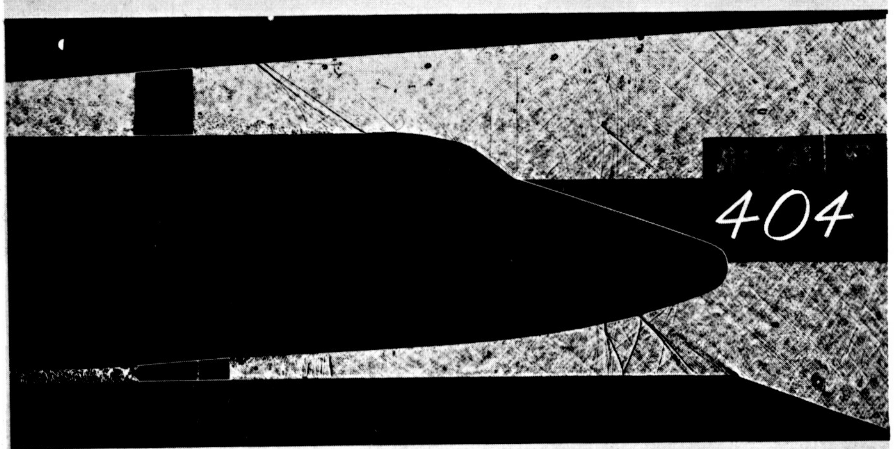

(b) $M_\infty = 1.10$, $q_\infty = 560$ psf

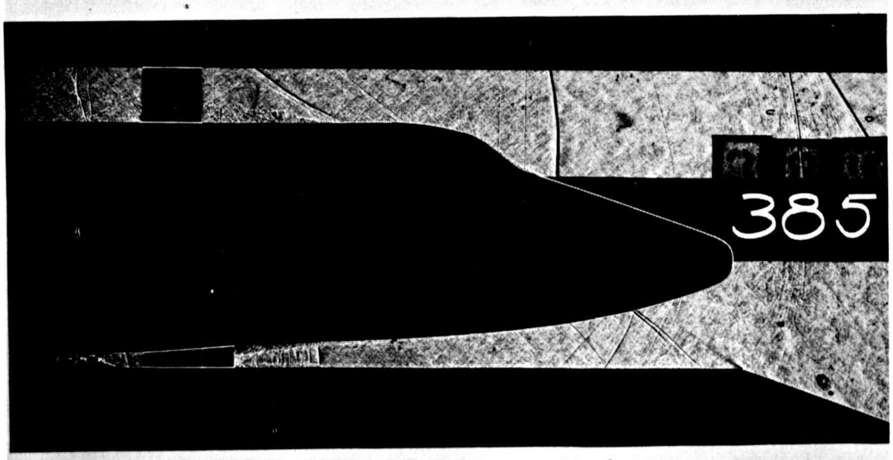

(c) $M_\infty = 1.30$, $q_\infty = 454$ psf

Figure 21. - Shadowgraphs of series-burn configuration 4 with both angle of attack and angle of sideslip equal to 0°.

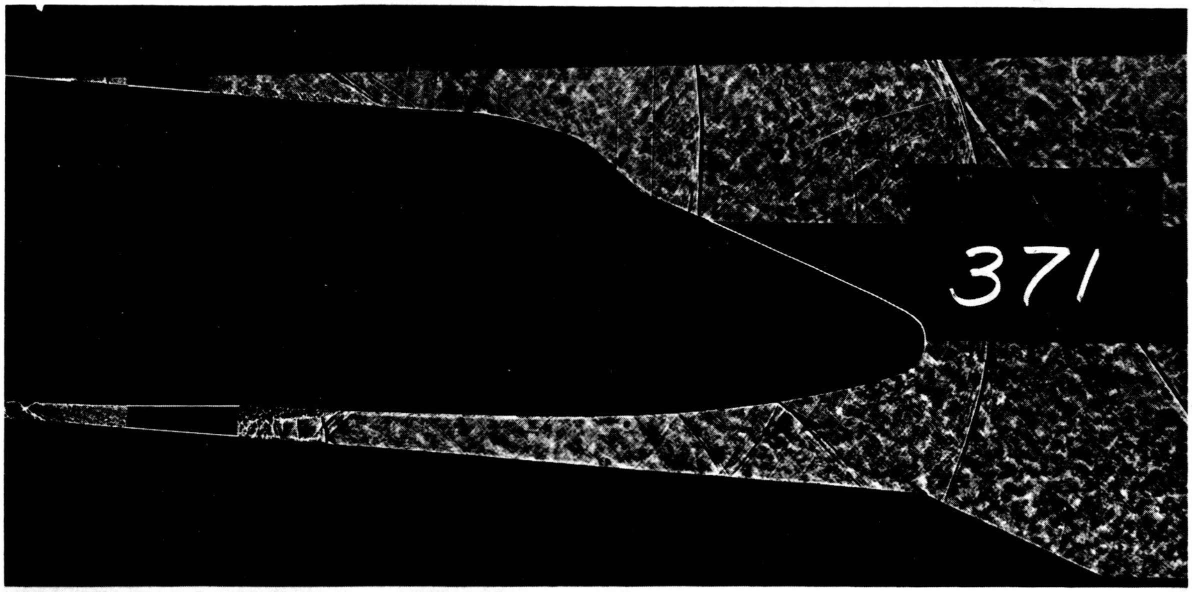

(a) $\alpha = -4°$, $\beta = 5°$, $q_\infty = 459$ psf

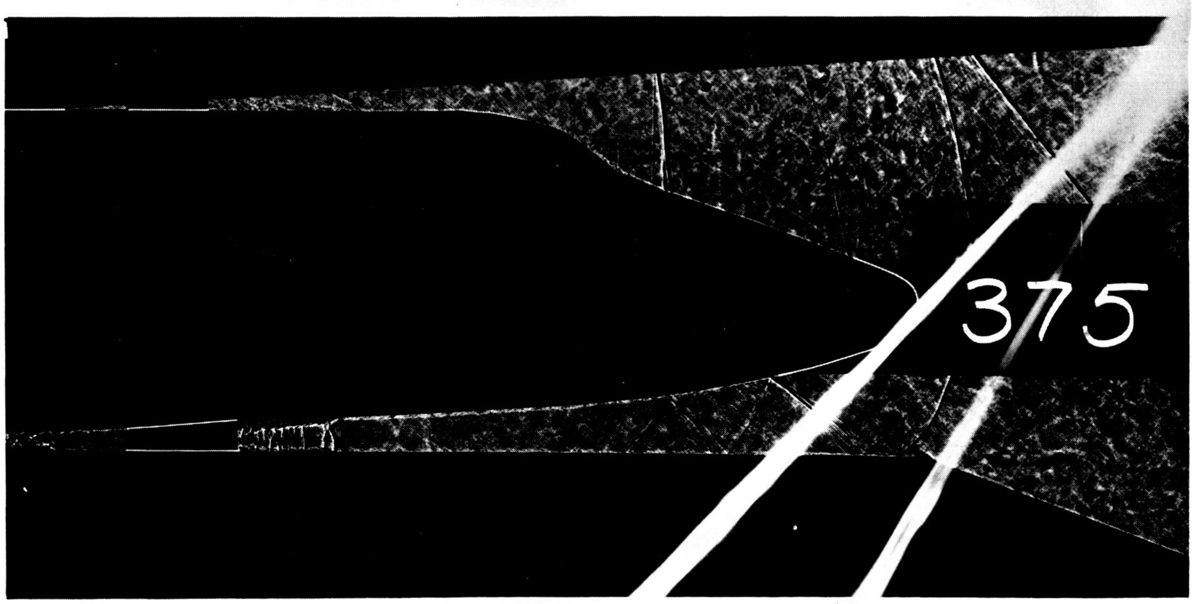

(b) $\alpha = 0°$, $\beta = 5°$, $q_\infty = 459$ psf

Figure 22. - Shadowgraphs of series-burn configuration 4 at $M_\infty = 1.40$.

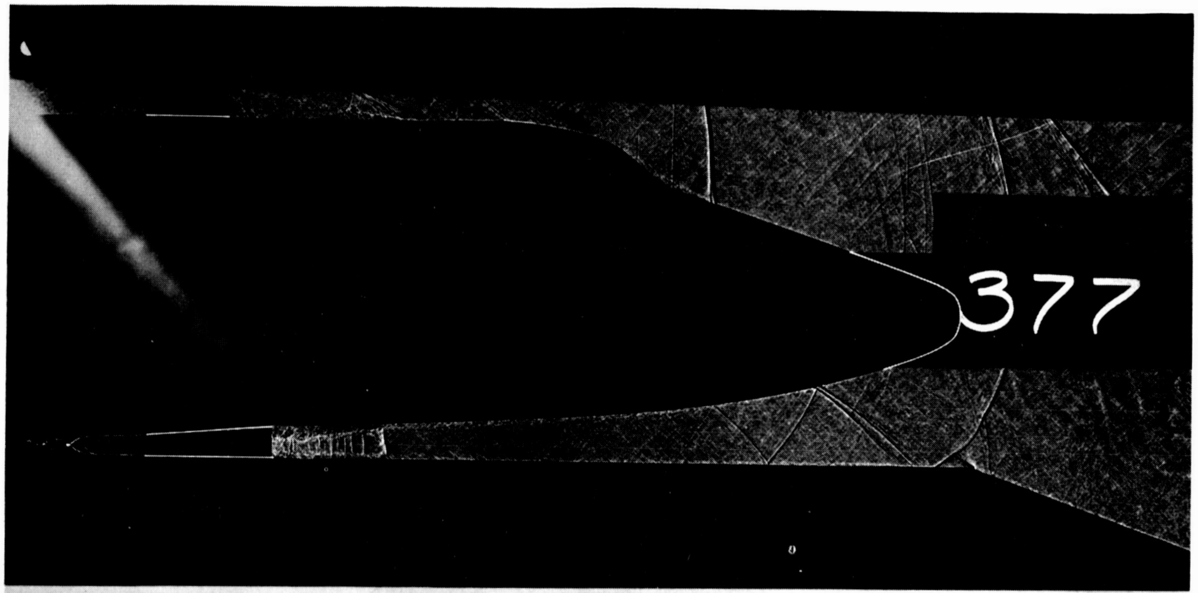

(c) $\alpha = 0°$, $\beta = 0°$, $q_{\infty} = 458$ psf

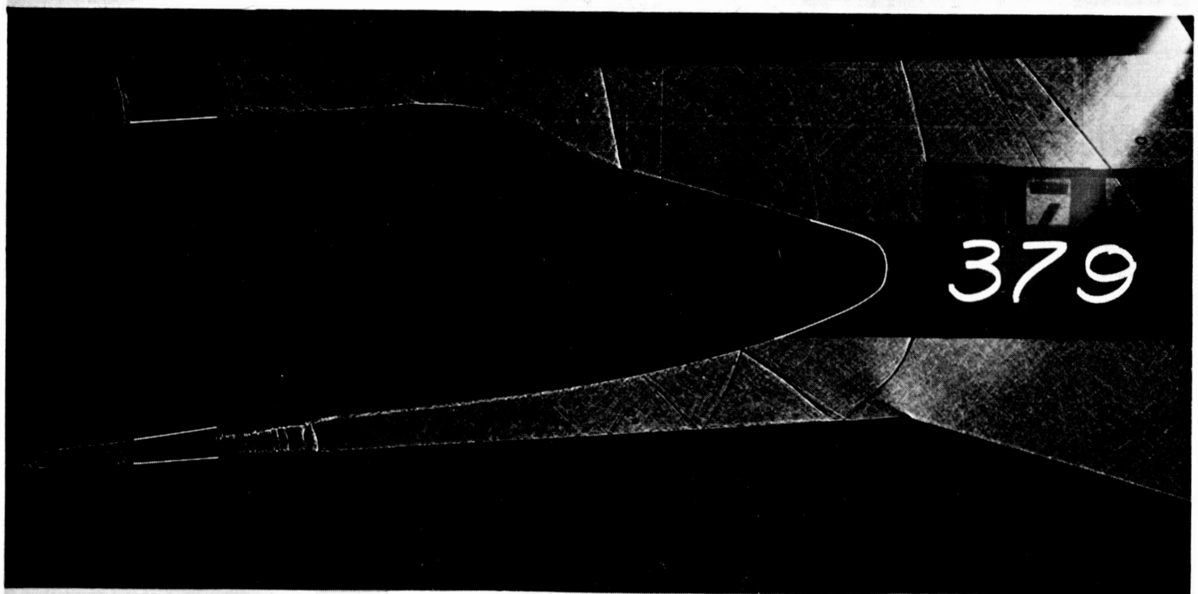

(d) $\alpha = 4°$, $\beta = 5°$, $q_{\infty} = 459$ psf

Figure 22. - Concluded.

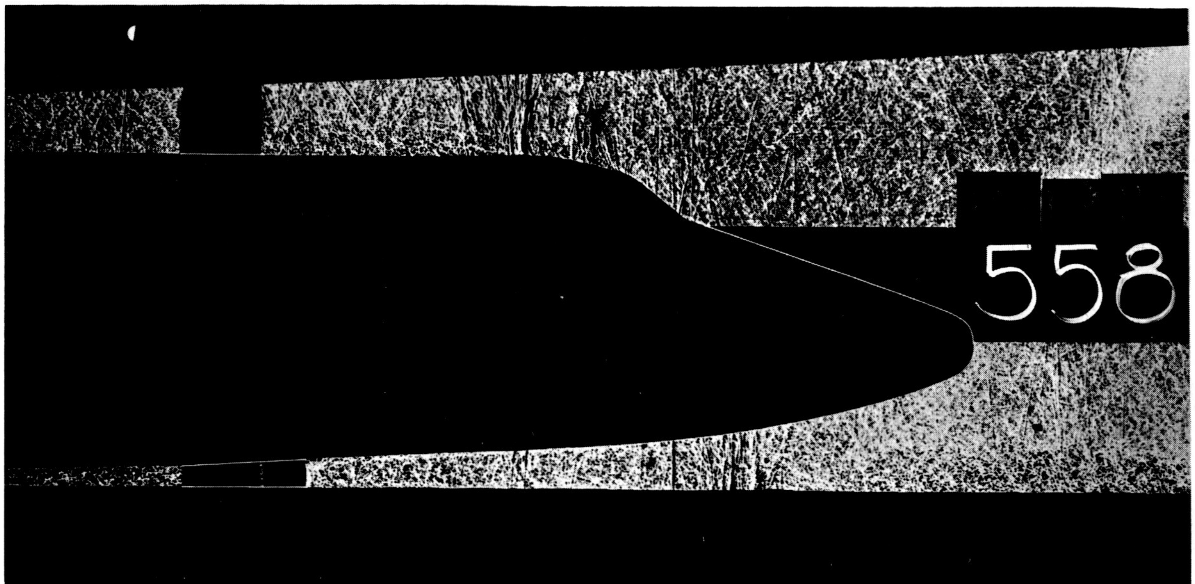

(a) $M_\infty = 0.80$, $q_\infty = 798$ psf

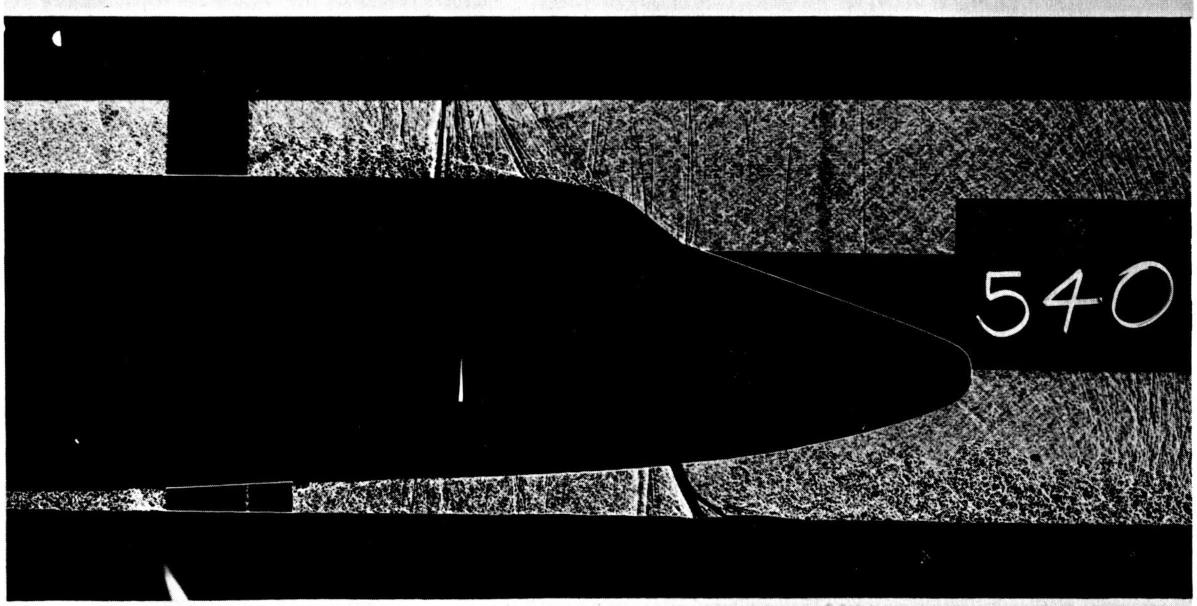

(b) $M_\infty = 0.90$, $q_\infty = 711$ psf

Figure 23. - Shadowgraphs of parallel-burn configuration 5 with both angle of attack and angle of sideslip equal to 0°.

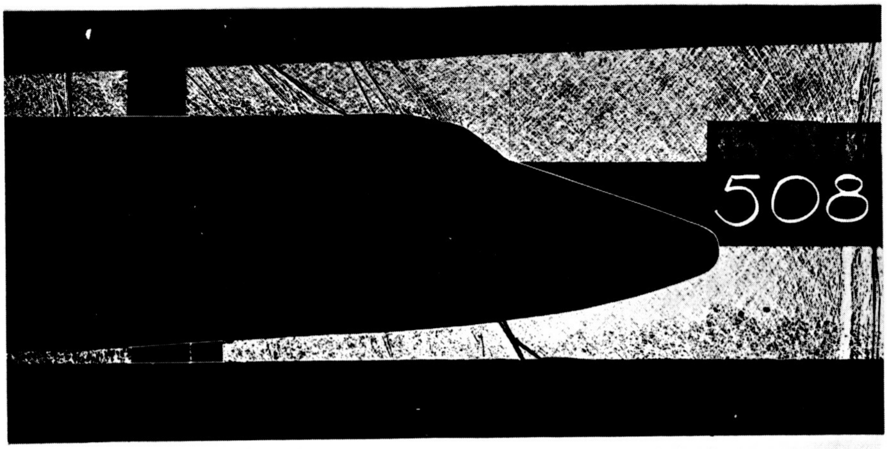

(c) $M_{\infty} = 1.00$, $q_{\infty} = 786$ psf

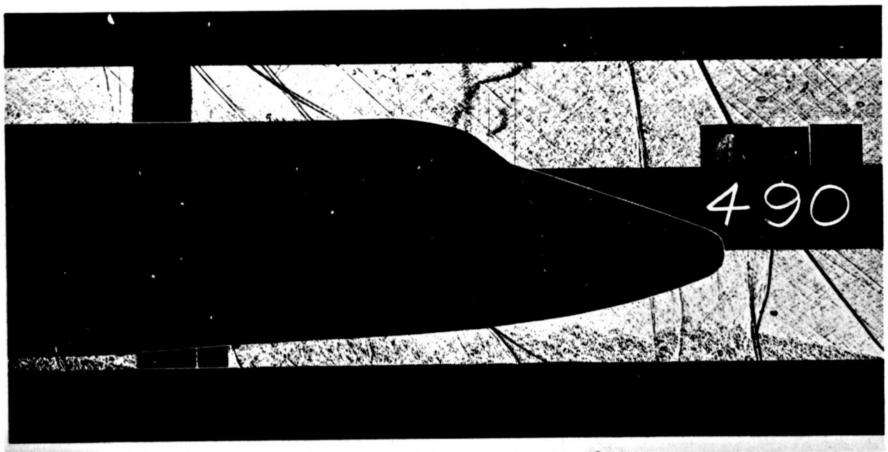

(d) $M_{\infty} = 1.20$, $q_{\infty} = 587$ psf

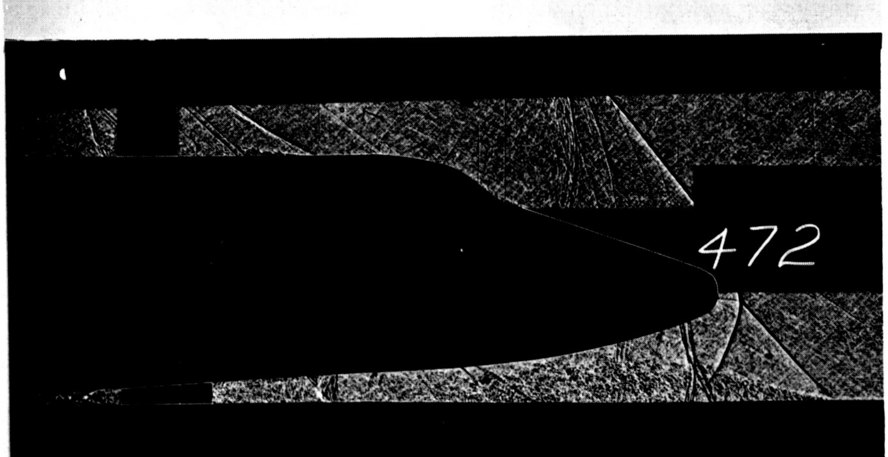

(e) $M_{\infty} = 1.40$, $q_{\infty} = 459$ psf

Figure 23. - Concluded.

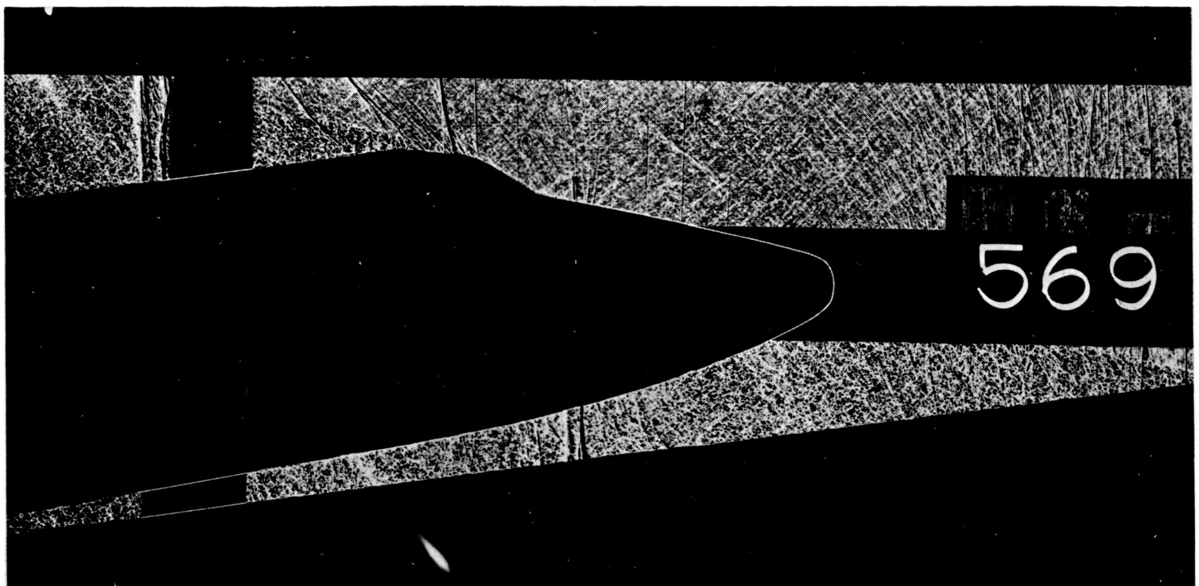

(a) $M_\infty = 0.95$, $q_\infty = 750$ psf

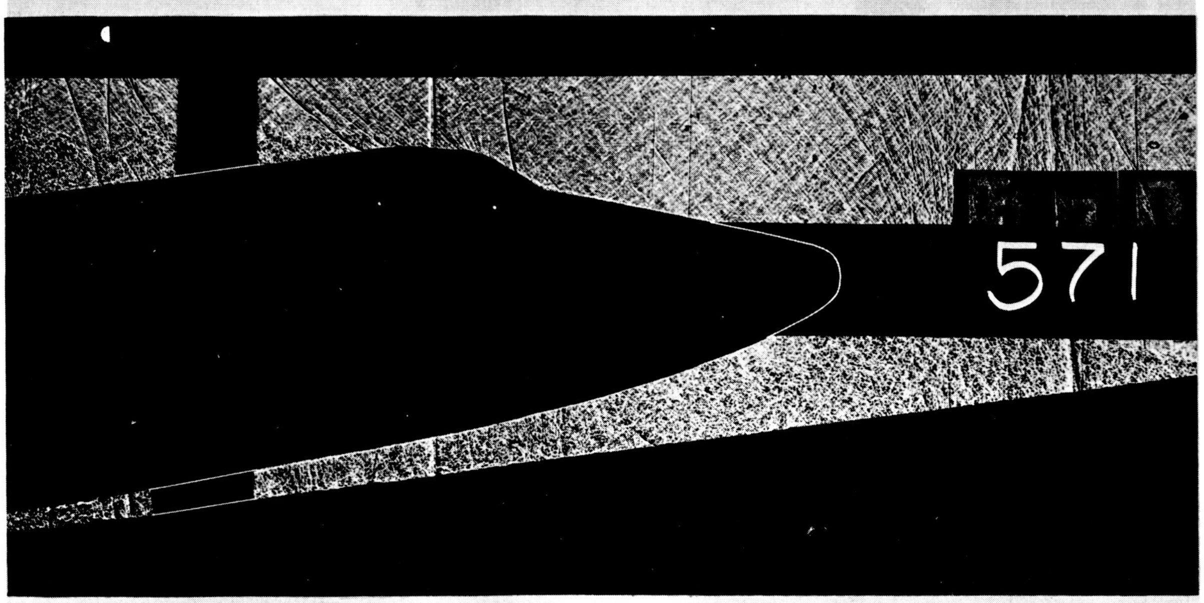

(b) $M_\infty = 1.00$, $q_\infty = 784$ psf

Figure 24. - Shadowgraphs of parallel-burn configuration 5 with angle of attack equal to 8° and angle of sideslip equal to -5°.

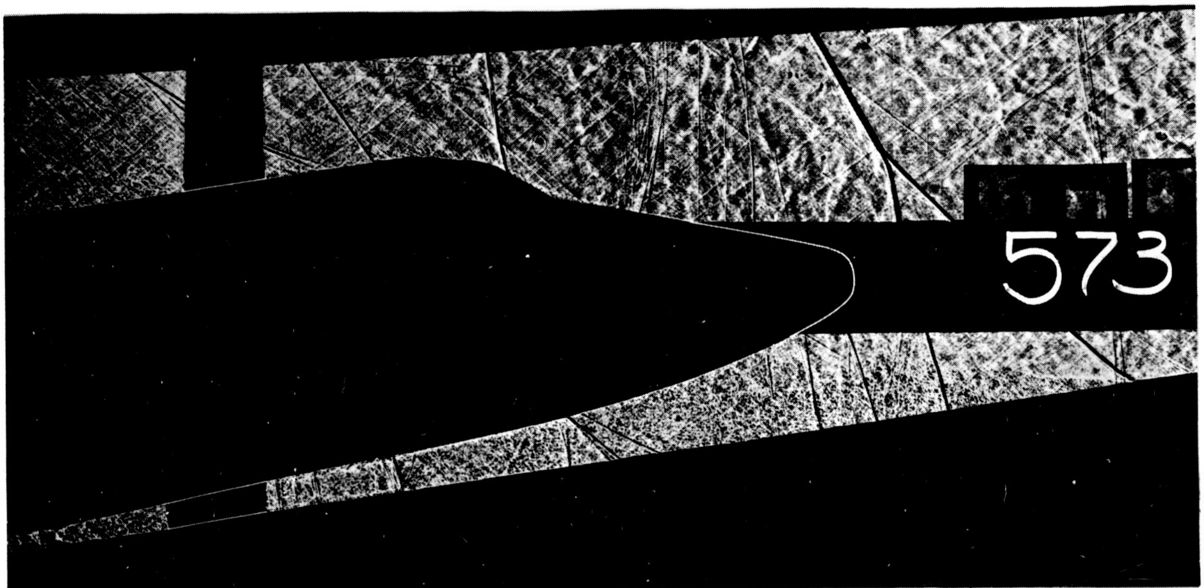

(c) $M_\infty = 1.20$, $q_\infty = 586$ psf

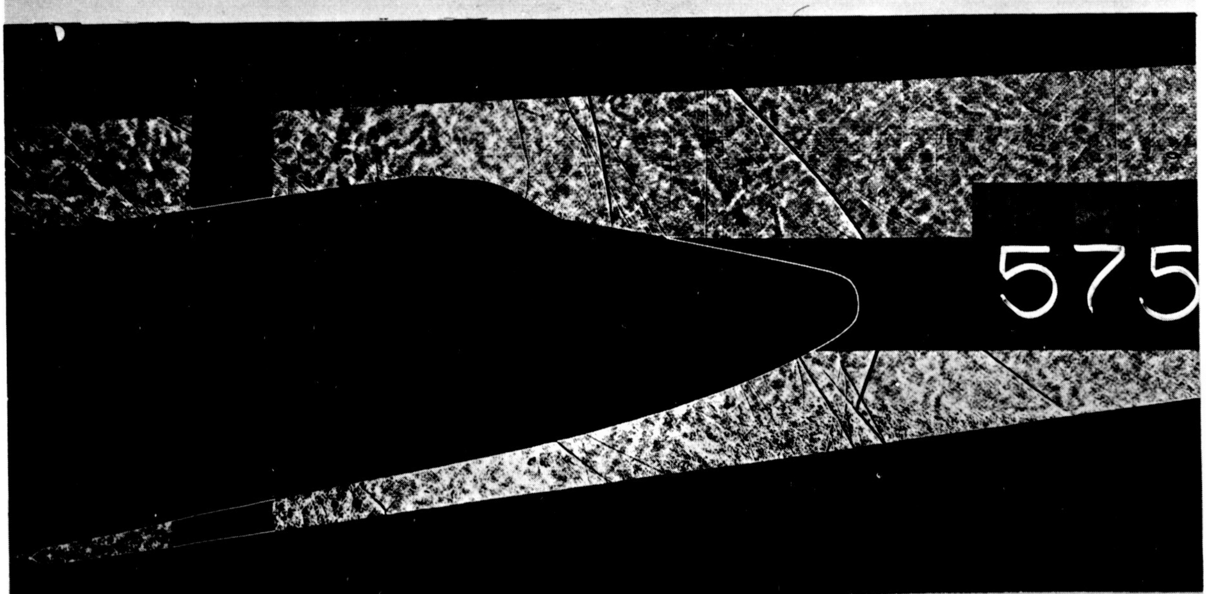

(d) $M_\infty = 1.40$, $q_\infty = 459$ psf

Figure 24. - Concluded.

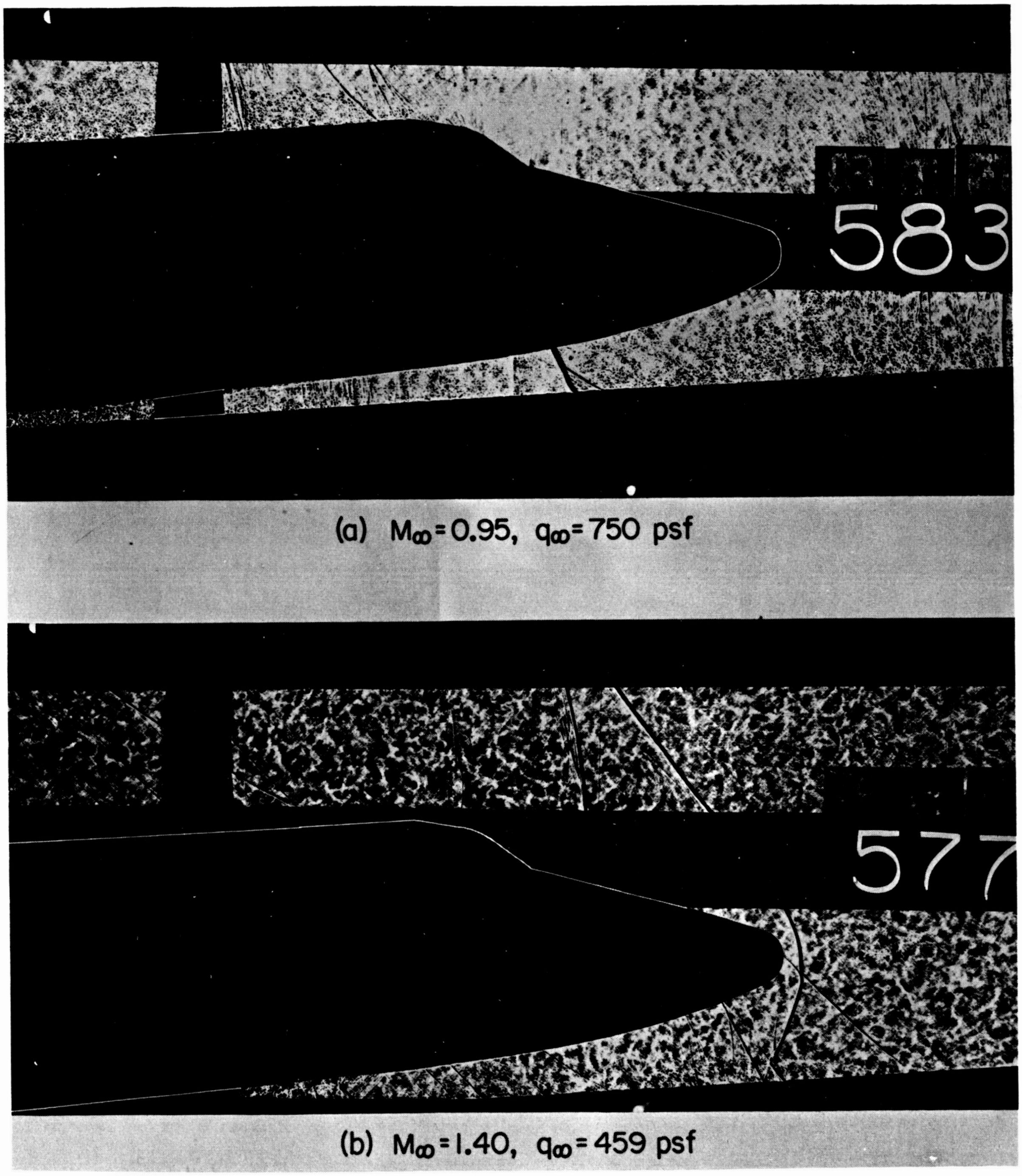

Figure 25. - Shadowgraphs of parallel-burn configuration 5 with angle of attack equal to 4° and angle of sideslip equal to -5°.

1. Report No. NASA TM X-62,444	2. Government Accession No.	3. Recipient's Catalog No.
4. Title and Subtitle Shadowgraphs of Air Flow over Prospective Space Shuttle Configurations at Mach Numbers From 0.8 to 1.4		5. Report Date May 1975
		6. Performing Organization Code
7. Author(s) Jules B. Dods, Jr., Richard D. Hanly and James H. Efting		8. Performing Organization Report No. A-6099
9. Performing Organization Name and Address Ames Research Center Moffett Field, Ca. 94035		10. Work Unit No. 506-17-32
		11. Contract or Grant No.
12. Sponsoring Agency Name and Address National Aeronautics and Space Administration Washington, D.C. 20546		13. Type of Report and Period Covered Technical Memorandum
		14. Sponsoring Agency Code
15. Supplementary Notes		

16. Abstract

Shadowgraphs of five Space Shuttle Launch configurations are presented. The model was a 4 percent-scale Space Shuttle Vehicle, tested in the 11- by 11-foot Transonic Wind Tunnel at Ames Research Center. The Mach number was varied from 0.8 to 1.4 with three angles of sideslip (0°, 5° and -5°) that were used in conjunction with three angles of attack (4°, -4°, and 0°). The model configurations included both series-burn and parallel-burn configurations, two canopy configurations, two positions of the Orbiter nose relative to the HO tank nose, and two HO tank nose-cones angles (15° and 20°). The data consist entirely of shadowgraph photographs.

17. Key Words (Suggested by Author(s)) Space Shuttle Vehicle Shadowgraphs		18. Distribution Statement Unclassified-Unlimited Star Category 15,02	
19. Security Classif. (of this report) Unclassified	20. Security Classif. (of this page) Unclassified	21. No. of Pages 51	22. Price* $3.75

*For sale by the National Technical Information Service, Springfield, Virginia 22151